Robust Design of Countercurrent Adsorption Separation Processes: 2. Multicomponent Systems

Marco Mazzotti, Giuseppe Storti, and Massimo Morbidelli
Dipartimento di Chimica Fisica Applicata, Politecnico di Milano, 20133 Milano, Italy

The adsorption separation of a multicomponent mixture in a four-section countercurrent separation unit is analyzed. A procedure for the optimal and robust design of the unit is developed in the frame of equilibrium theory, where adsorption equilibria are described through the constant selectivity stoichiometric model, while mass-transfer resistances and axial dispersion are neglected.

A set of conditions obtained defines a region in the operating parameters space where the unit achieves complete separation. In the case of binary separations, with a desorbent having any adsorptivity with respect to the components to be separated, the boundaries of this region are obtained explicitly. In the general multicomponent case, a numerical procedure is needed. An approximate shortcut method devised allows to obtain explicit and reliable relationships for estimating the boundaries of the exact region.

The results provide a very convenient tool not only to analyze the role of the desorbent in determining the separation performance, but to find both optimal and robust operating conditions. Comparison between model predictions and experimental data assesses the reliability and accuracy of the theoretical findings.

Introduction

Continuous countercurrent units are used widely for the adsorption separation of multicomponent mixtures (cf. Ruthven, 1984; Ganetsos and Barker, 1993). The typical scheme of a so-called true countercurrent (TCC) unit is presented in Figure 1. Depending on the operating conditions, the most adsorbable components of the feed stream are collected in the extract stream, whereas the least adsorbable ones are collected in the raffinate stream. A desorbent stream is also needed to regenerate the adsorbent and improve the separation.

In practice, the countercurrent contact between the fluid and solid phases can be conveniently achieved in a simulated moving bed (SMB) apparatus where the solid beds are fixed, while the locations of the inlet and outlet ports undergo a discrete movement in the same direction as the fluid stream. Since the Sorbex process was developed by UOP (cf. Broughton and Gerhold, 1961; Johnson and Kabza, 1993), several applications have been reported in the literature. These are typically concerned with the liquid-phase separations in units with a large number of columns to closely mimic the continuous movement of the solid (cf. Ruthven and Ching, 1989). Recently, an ap-

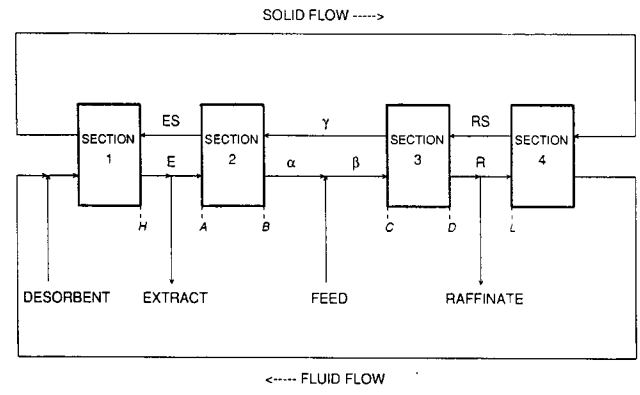

Figure 1. Four-section true countercurrent unit for adsorption separation.

The symbols identify different streams. The labels attached to the column ends indicate the sections where material balances are considered.

Correspondence concerning this article should be addressed to M. Morbidelli.
The first part of this series was presented by Storti et al. (1993a).
G. Storti is presently at the Dipartimento di Chimica Inorganica, Metallorganica e Analitica, Università degli Studi di Padova, Via Marzolo, 1, 35131 Padova, Italy.

plication referring to a SMB pilot plant with only six ports and operating in the vapor phase has been reported (Storti et al., 1992, 1993b).

The equivalence between TCC and SMB units has been extensively used for modeling and design purposes (cf. Ruthven and Ching, 1989). In general, it is convenient to use TCC simulation models since their stationary regime is time-independent. On the contrary, a SMB unit in the stationary regime has a cyclic behavior, due to the periodic movement of the feed and withdrawal points through the sequence of columns.

The successful design and operation of countercurrent separation units depend on the correct selection of the operating conditions, particularly of the flow rate values in each section. Because of the complex behavior of these units, such a selection is not straightforward and several procedures have been proposed in the literature to guide their optimal design. Some of these, based on the approximation of the unit as a sequence of equilibrium stages and then on the application of a McCabe-Thiele-like analysis, have been reviewed by Ruthven (1984) and more recently by Hashimoto et al. (1993). An alternative approach is based on the equilibrium theory model, which takes into account the nonlinearity of the adsorption equilibria, whereas it neglects the effect of axial mixing and mass-transport resistances (Helfferich and Klein, 1970; Rhee et al., 1971; Storti et al., 1989). This model has provided a very useful tool for the qualitative simulation of adsorption separation units, since in several instances it has been shown that the dynamic behavior of these units is affected strongly by the nonlinearities involved in the adsorption equilibria (cf. Paludetto et al., 1987a,b). The equilibrium theory model of the generic jth section of the TCC unit in Figure 1 is given by the following set of first-order hyperbolic partial differential equations:

$$\frac{\partial}{\partial \tau}[\epsilon^* y_i^j + (1-\epsilon^*)\sigma\theta_i^j] + (1+\epsilon_p)\sigma\frac{\partial}{\partial x}[m_j y_i^j - \theta_i^j] = 0 \qquad (i=1, \ldots, NC), \quad (1)$$

where:

$$\theta_i^j = f_i^{eq}(\mathbf{y}^j) \quad (i=1, \ldots, NC). \quad (2)$$

The boundary conditions are given by:

$$\begin{aligned} y_i^j(\tau, 0) &= (y_i^j)^a \quad (i=1, \ldots, NC) \\ \theta_i^j(\tau, 1) &= (\theta_i^j)^b \quad (i=1, \ldots, NC) \\ y_i^j(0, x) &= (y_i^j)^o \quad (i=1, \ldots, NC), \end{aligned} \quad (3)$$

where y_i and θ_i represent the fluid and adsorbed-phase concentrations, respectively.

To model a countercurrent unit with four sections, we consider the above system once for each section: Eqs. 1 to 3 with $j=1, \ldots, 4$, together with the mass balances at the nodes connecting the neighboring sections. Above equations show that, in the framework of equilibrium theory and being the physical properties of the system (ϵ^*, σ and the equilibrium parameters) fixed, the steady-state behavior of the countercurrent units is determined only by the values of the mass-flow rate ratios m_j. These are defined as the ratio between the net fluid mass-flow rate and the adsorbed-phase mass-flow rate in each section of the unit:

$$m_j = \frac{\text{net fluid mass-flow rate}}{\text{adsorbed phase mass-flow rate}} = \frac{u_j\rho_f - u_s\epsilon_p\rho_f}{u_s\rho_s\Gamma^\infty(1-\epsilon_p)}, \quad (4)$$

where the net fluid flow rate is evaluated as the difference between the total fluid flow rate and the flow rate of the fluid inside the macropores carried in the opposite direction by the solid. The design problem is then reduced to the estimation of m_j values which optimize the separation performance.

In Part 1 of this series (Storti et al., 1993a), the equilibrium theory model has been used to design the operating conditions for the separation of a binary mixture, in the case where the adsorptivity of the desorbent is intermediate between those of the two components to be separated. In particular, a set of explicit relationships representing the boundaries of the region corresponding to complete separation conditions in the operating parameter space has been derived. Based on this complete separation region, optimal and robust operating conditions can be determined.

In spite of the simplicity of its construction and use, the complete separation region has proved effective in giving information about the operation and performance of continuous countercurrent separation units. Therefore, in this work we extend the approach and the results presented in Part 1 to the adsorption separation of a multicomponent mixture in a four-section unit, using a desorbent having any adsorptivity value with respect to that of the species to be separated.

First, from material balance considerations we derive necessary conditions for complete separation. Next, by analyzing the behavior of each section of the unit with respect to the neighboring ones in the framework of equilibrium theory, a set of constraints on the operating parameters, the mass-flow rate ratios m_j, $j=1, \ldots, 4$, is derived. From these, using a step-by-step procedure for solving the equilibrium theory model in each section of the unit, we determine the steady-state composition of all the involved streams. In general a numerical procedure is required to determine the region of complete separation in the space of the operating parameters. It is worth noting that this analysis is valid for all the values of the adsorptivity of the desorbent with respect to that of the components to be separated. Exact relationships for the boundaries of the complete separation region in the case of binary separation with weak or strong desorbent, that is, a desorbent having smaller or greater adsorptivity than that of the two components to be separated, are obtained. In the case of a binary separation with intermediate desorbent, the obtained results reduce to those presented in Part 1. The effect of the desorbent adsorptivity on the performance of a binary separation unit is discussed.

Then, we derive the complete separation region for multicomponent mixtures following the approach presented in the previous sections. A shortcut procedure based on the concept of strong-key and weak-key components is also developed. This allows to reduce the multicomponent separation to an equivalent binary separation, for which the complete separation region can be determined analytically. The exact region obtained numerically is compared with the approximate region obtained through the shortcut procedure. Finally, the theoretical results are compared with a set of experimental data obtained in a six-port SMB pilot unit operated in the vapor

phase for the separation of mixtures of the alkylaromatic C-8 fraction.

Complete Separation

The requirement of complete separation for a NC-component mixture in the four-section countercurrent unit in Figure 1 implies that the components of the mixture can be divided in two different groups. The first one (E) includes the strongly adsorbable components which are collected in the extract stream, whereas the second (R) includes the weakly adsorbable components which are collected in the raffinate stream. Thus, the species in group E are absent from the raffinate stream, whereas those in group R are absent from the extract stream. In principle, this separation can be achieved using any desorbent, having any adsorptivity value with respect to that of the components to be separated, provided that proper operating conditions are selected. In this work, we derive exact criteria to perform this selection in the case of constant selectivity stoichiometric systems, characterized by the following adsorption equilibrium model:

$$\theta_i = \frac{K_i y_i}{\sum_{j=1}^{NC} K_j y_j}. \tag{5}$$

This relationship is very useful in describing various systems of interest in applications, since it accounts for the competition toward adsorption among the various species in the fluid mixture, as well as for the upper limit to the overall adsorbable amount of mass imposed by the adsorbent saturation conditions.

We list all the components, including the desorbent, D, in the increasing order of adsorptivity: in increasing values of their equilibrium constant K_i ($i=1, \ldots, NC$). The set E includes NE species with $K_i \geq K_{sk}$, where the subscript sk indicates the *strong-key component*: the weakest component among those to be collected in the extract stream. Similarly, the set R includes NR species with $K_i \leq K_{wk}$, where wk indicates for the *weak-key component*: the strongest component among those to be collected in the raffinate stream. Thus, when neglecting the desorbent, we have $K_1 < K_2 < \ldots < K_{wk} < K_{sk} < \ldots < K_{NC}$. Various cases may arise depending on the desorbent adsorptivity value. We refer to an intermediate desorbent when $K_{wk} < K_D < K_{sk}$, hence $wk = D-1$ and $sk = D+1$. On the other hand, we define the adsorbent to be a strong intermediate when $K_{sk} < K_D < K_{NC}$, and strong when it is stronger than all the components to be separated, so that $D = NC$ and $K_D > K_i$ for $i = 1, \ldots, NC-1$. Similarly, the desorbent is a weak intermediate when $K_1 < K_D < K_{wk}$ and weak when it is weaker than all the components to be separated, so that $D = 1$ and $K_D < K_i$ for $i = 2, \ldots, NC$. For brevity, in the following we indicate the weakest component in R with the subscript ww: $ww = 1$ always and $ww = 2$ when the desorbent is weak. On the other hand, subscript ss indicates the strongest component in E: $ss = NC$ always and $ss = NC-1$ when the desorbent is strong. Finally, note that $NC = NE + NR + 1$. Table 1 shows the classification of various systems according to the relative adsorption strength of desorbent. Note that the same notation and classification can also be used for linear systems described by the linear adsorption isotherm $\theta_i = K_i y_i$.

Main results of equilibrium theory relevant to the subsequent treatment are summarized in Appendix A. At steady state a constant state prevails in each section of the unit. According to the definition of the mass-flow rate ratios m_j given by Eq. 4, the net flow rate of the ith component in the jth section of the unit is proportional to the quantity f_i^j, defined by $f_i^j = m_j y_i^j - \theta_i^j$.

Complete separation requires that in each section of the unit the net flow rates of the strong components, which belong to E, are negative, so that they are conveyed toward the extract outlet. Similarly, the net flow rates of the weak components in the set R must be positive, so that they are carried toward the raffinate outlet. This specifies the sign, positive or negative, of the variables f_i^j. Thus, the following inequalities in terms of the mass-flow rate ratios m_j are obtained:

$$\begin{aligned}
&\text{Section 1:} && m_1 > \theta_i^1/y_i^1, && i \in E \cup R \\
&\text{Section 2:} && m_2 < \theta_i^2/y_i^2, && i \in E \\
& && m_2 > \theta_i^2/y_i^2, && i \in R \\
&\text{Section 3:} && m_3 < \theta_i^3/y_i^3, && i \in E \\
& && m_3 > \theta_i^3/y_i^3, && i \in R \\
&\text{Section 4:} && m_4 < \theta_i^4/y_i^4, && i \in E \cup R.
\end{aligned} \tag{6}$$

Introducing the parameter δ_j defined as the denominator of the adsorption equilibrium model (Eq. 5) corresponding to the steady constant state in section j:

$$\delta_j = \sum_{l=1}^{NC} K_l y_l^j \quad (j = 1, \ldots, 4), \tag{7}$$

the conditions in Eqs. 6 reduce to:

$$\begin{aligned}
&\text{Section 1:} && K_{ss} < m_1 \delta_1 < +\infty \\
&\text{Section 2:} && K_{wk} < m_2 \delta_2 < K_{sk} \\
&\text{Section 3:} && K_{wk} < m_3 \delta_3 < K_{sk} \\
&\text{Section 4:} && -\frac{\epsilon_p \delta_4}{\sigma(1-\epsilon_p)} < m_4 \delta_4 < K_{ww}.
\end{aligned} \tag{8}$$

Table 1. Classification of NC-Component Systems Depending on the Relative Adsorption Strength of the Desorbent*

Desorbent Type	Desorbent Index	Species in Set E	Species in Set R	$(sk - wk)$
Weak	$D=1$	$2, \ldots, wk$	$sk, \ldots, NC$	1
Weak-intermediate	$1<D<wk$	$1, \ldots, D-1, D+1, \ldots, wk$	$sk, \ldots, NC$	1
Intermediate	$wk<D<sk$	$1, \ldots, wk$	$sk, \ldots, NC$	2
Strong-intermediate	$sk<D<NC$	$1, \ldots, wk$	$sk, \ldots, D-1, D+1, \ldots, NC$	1
Strong	$D=NC$	$1, \ldots, wk$	$sk, \ldots, NC-1$	1

*D = desorbent; wk = weak-key component; sk = strong-key component. The mixture to be separated includes $(NC-1)$ components.

Note that m_4 can have negative values for positive fluid flow rates, as can be seen from the definition of the mass-flow rate ratio (Eq. 4). From a physical point of view, this situation represents the extreme case where the flow rate of the fluid carried in the moving solid macropores is greater than the fluid flow rate itself.

The case of a system characterized by a linear adsorption isotherm can be regarded as a particular case of the constant selectivity system (Eq. 5), where $\delta_j = 1$, for $j = 1, \ldots, 4$. In this case, the inequalities (Eqs. 8) become explicit and define a region in the four-dimensional space having the operating parameters m_1, m_2, m_3, and m_4 as coordinates. The points within this region represent operating conditions corresponding to complete separation. Note that these conditions depend neither on the feed composition nor on the adsorptivity strength of the desorbent.

Let us consider the two central sections of the Sorbex unit, which have a crucial role in the separation performance of the unit. Since m_3 must be greater than m_2 to have a positive feed flow rate, in the case of linear adsorption equilibria the constraints in Eqs. 8 on m_2 and m_3 reduce to:

$$K_{wk} < m_2 < m_3 < K_{sk}. \tag{9}$$

These inequalities define the projection onto the $m_2 - m_3$ plane of the four-dimensional region corresponding to complete separation. It is worth noting that the projected region does not depend on the net flow ratios in sections 1 and 4. Accordingly, it can be concluded that any pair of (m_2, m_3) values which lies within this triangular region in the $m_2 - m_3$ plane leads, in the framework of equilibrium theory, to complete separation performance, as long as the values of m_1 and m_4 are selected to satisfy the corresponding conditions in Eqs. 8.

The situation is much more complicated in the case of a nonlinear system, since conditions 8 are implicit. Each variable δ_j, $j = 1, \ldots, 4$, depends in fact on the whole set of operating parameters m_j. In particular, δ_j depends on the constant state in section j, which according to equilibrium theory (cf. Appendix A) is a function of m_j and of the two states entering the column, which in turn depend on the behavior of the neighboring sections and then on the flow rate ratios m_{j-1} and m_{j+1}.

Moreover, conditions 8 are necessary, but not sufficient. They deal only with the behavior of each section separately, ignoring the interaction with other sections of the unit and the compatibility conditions which may arise from this interaction.

To determine sufficient conditions for complete separation, we need to further elaborate the above inequalities using equilibrium theory. First, we must find out which configuration of the four-section separation unit is compatible with the requirement of complete separation, with conditions 8. It can be proved that in each section of the unit only one configuration is consistent with this requirement. This does not mean that only one specific constant state can be chosen, but rather that the *kind* of constant state compatible with complete separation is unique. In other words, only a constant state identified by a specific index k (see Eq. A9 in Appendix A) can prevail at steady state in each section.

This result, which is the basis for the quantitative analysis developed in the next sections, is stated in the following complete separation proposition, which is proved in Appendix B for the general case of a NC-component system with desorbent having any adsorptivity value (see Figure 1 for the symbols identifying the various streams in the unit).

Theorem 1: complete separation proposition

Necessary and sufficient condition to obtain complete separation is that the constant states prevailing in each section are those reported in the third column of Table 2, with the relevant vector of Ω values as in the second column. The Ω parameters with superscript E, ES, γ, R, RS, β are as yet undetermined values. They must fulfill the inequality:

$$\min\{\Omega_i^D, \Omega_i^F\} \le \Omega_i \le \max\{\Omega_i^D, \Omega_i^F\}, \tag{10}$$

for $i = 1, \ldots, NC-1$. To obtain the desired constant state in each section, the values of the corresponding net flow rate ratios must fall in the interval reported in the last column of Table 2.

It is noteworthy that the kind of constant state that prevails in each section of the unit does not depend on the adsorptivity of the desorbent. Table 2 shows that the fluid state prevails in section 1 ($k = NC-1$), whereas the solid state prevails in section 4 ($k = 0$). For all values of the desorbent adsorptivity, in both sections 2 and 3 the steady constant state is identified by $k = NR$, where NR is the number of components in the feed mixture to be collected in the raffinate stream. On the other hand, the ranges of admittable m_j values depend on the adsorptivity of the desorbent, as indicated in the last column of Table 2.

Design of Operating Conditions to Achieve Complete Separation

The conditions derived in the previous section impose a unique range of values for the m_j parameters of a four-section separation unit. These could be used to choose the proper operating conditions with a trial-and-error procedure based on iterative simulations of the separation unit behavior. In this section we solve the design problem directly. The aim is to determine the value of the flow rate ratio m_j in each section of the unit which allows to achieve complete separation.

Storti et al. (1989) provided the solution of the equilibrium theory model of a four-section continuous countercurrent adsorption separation unit in the most general case. Here, we consider a reduced set of equations which applies only to the case where complete separation is achieved, thus accounting for the conditions in Table 2.

As mentioned above, the $[4 \times (NC-1)]$ Ω values characterizing the streams E, ES, α, β, γ, R and RS in Table 2 are as yet unknown. Moreover, the four flow rate ratios, m_1, m_2, m_3, and m_4, and the fluid flow rates of the feed, fresh desorbent, extract and raffinate streams are to be determined. These unknowns must satisfy $(4 \times NC)$ overall and single-component material balances at the ends of the columns and at the nodes of the unit. The balance of equations and unknowns leave 4 degrees of freedom, which are most conveniently chosen as the four flow rate ratios, m_1, m_2, m_3, and m_4. Note that in the model equations we use the superficial flow rate ratio $\mu_j = u_s/u_j$, which can be expressed in terms of m_j through Eq. 4.

For Figure 1 the following mass balances are considered.

Table 2. Ω Vectors Compatible with the Requirement of Complete Separation, Constant State Prevailing at Steady Conditions and Corresponding Range of m_j Values for Each Stream in the Unit as in Figure 1*

Stream	Ω Vector	State	Desorbent	m Range
1	$K_{ww}, \ldots, K_{ss}$	$NC-1$	$D<NC$	$K_{NC}/K_D<m_1<+\infty$
			$D=NC$	$\Omega^{ES}_{NC-1}/K_D<m_1<+\infty$
E	$K_{ww}, \ldots, K_{wk}, \Omega^{E}_{NR+1}, \ldots, \Omega^{E}_{NC-1}$	—	any	—
ES	$K_{ww}, \ldots, K_{wk}, \Omega^{ES}_{NR+1}, \ldots, \Omega^{ES}_{NC-1}$	—	any	—
2	$K_{ww}, \ldots, K_{wk}, \Omega^{\gamma}_{NR+1}, \ldots, \Omega^{\gamma}_{NC-1}$	$wk-1=NR$	$D<wk$	$K_{wk}<m_2\delta_2<\Omega^{\gamma}_{NR+1}$
		$wk=NR$	$wk<D<sk$	$\Omega^{\gamma}_{NR}<m_2\delta_2<\Omega^{\gamma}_{NR+1}$
		$wk=NR$	$D>sk$	$\Omega^{\gamma}_{NR}<m_2\delta_2<K_{sk}$
α	$\Omega^{\alpha}_{1}, \ldots, \Omega^{\alpha}_{NR}, \Omega^{\gamma}_{NR+1}, \ldots, \Omega^{\gamma}_{NC-1}$	—	any	—
β	$\Omega^{\gamma}_{1}, \ldots, \Omega^{\gamma}_{NR}, \Omega^{\beta}_{NR+1}, \ldots, \Omega^{\beta}_{NC-1}$	—	any	—
γ	$\Omega^{\gamma}_{1}, \ldots, \Omega^{\gamma}_{NC-1}$	—	any	—
3	$\Omega^{\gamma}_{1}, \ldots, \Omega^{\gamma}_{NR}, K_{sk}, \ldots, K_{ss}$	$wk-1=NR$	$D<wk$	$K_{wk}<m_3\delta_3<\Omega^{\beta}_{NR+1}$
		$wk=NR$	$wk<D<sk$	$\Omega^{\beta}_{NR}<m_3\delta_3<\Omega^{\beta}_{NR+1}$
		$wk=NR$	$D>sk$	$\Omega^{\beta}_{NR}<m_3\delta_3<K_{sk}$
R	$\Omega^{R}_{1}, \ldots, \Omega^{R}_{NR}, K_{sk}, \ldots, K_{ss}$	—	any	—
RS	$\Omega^{RS}_{1}, \ldots, \Omega^{RS}_{NR}, K_{sk}, \ldots, K_{ss}$	—	any	—
4	$K_{ww}, \ldots, K_{ss}$	0	$D>1$	$\frac{-\epsilon_p}{\sigma(1-\epsilon_p)}<m_4<K_1/K_D$
			$D=1$	$\frac{-\epsilon_p}{\sigma(1-\epsilon_p)}<m_4<\Omega^{R}_{1}/K_D$

*When indicating a set of K_i values, such as $K_n, \ldots, K_j$, we do not include K_D.

Overall mass balances at each node of the unit:

$$\frac{1}{\mu_D}=\sigma(1-\epsilon_p)(m_1-m_4) \tag{11}$$

$$\frac{1}{\mu_E}=\sigma(1-\epsilon_p)(m_1-m_2) \tag{12}$$

$$\frac{1}{\mu_F}=\sigma(1-\epsilon_p)(m_3-m_2) \tag{13}$$

$$\frac{1}{\mu_R}=\sigma(1-\epsilon_p)(m_3-m_4) \tag{14}$$

Mass balances of the strong components, $i \in E$

- Overall mass balance of component i:

$$\frac{1}{\mu_F}y_i^F=\frac{1}{\mu_E}y_i^E \tag{15}$$

- Mass balance of component i at boundary H:

$$y_i^E=\mu_1[\epsilon_p y_i^{ES}+(1-\epsilon_p)\sigma\theta_i^{ES}] \tag{16}$$

- Mass balance of component i at boundary A:

$$y_i^E-y_i^2(1-\epsilon_p\mu_2)=\mu_2[\epsilon_p y_i^{ES}+(1-\epsilon_p)\sigma(\theta_i^{ES}-\theta_i^2)] \tag{17}$$

- Mass balance of component i at boundary C:

$$y_i^{\beta}=\mu_3[\epsilon_p y_i^{\gamma}+(1-\epsilon_p)\sigma\theta_i^{\gamma}] \tag{18}$$

Mass balances for the weak components, $i \in R$

- Overall mass balance of component i:

$$\frac{1}{\mu_F}y_i^F=\frac{1}{\mu_R}y_i^R \tag{19}$$

- Mass balance of component i at boundary L:

$$y_i^R=\mu_4[\epsilon_p y_i^{RS}+(1-\epsilon_p)\sigma\theta_i^{RS}] \tag{20}$$

- Mass balance of component i at boundary G:

$$y_i^R-y_i^3(1-\epsilon_p\mu_3)=\mu_3[\epsilon_p y_i^{RS}+(1-\epsilon_p)\sigma(\theta_i^{RS}-\theta_i^3)] \tag{21}$$

- Mass balance of component i at boundary B:

$$y_i^{\alpha}=\mu_2[\epsilon_p y_i^{\gamma}+(1-\epsilon_p)\sigma\theta_i^{\gamma}] \tag{22}$$

Note that the above mass-balance equations have been derived under the assumption that complete separation has been achieved, hence they apply only in the case where the flow rate ratios fulfill the constraints in Table 2.

Solution of the Design Problem

For a given set of operating parameters, m_1, m_2, m_3, and m_4, the system of nonlinear equations (Eqs. 11 to 22) provides

the values of the variables Ω and δ_j through Eq. A8 in Appendix A, which appear in the expressions of the boundaries of the admittable intervals for m_j in Table 2. This allows us to check the fulfillment of these constraints by the given m_j values.

In principle, the above conditions could be written in terms only of the operating parameters m_j, thus defining a region of complete separation in the operating parameter space. This was done in Part 1 in the case of a binary separation with intermediate desorbent, for which explicit expressions for the boundaries of this region were reported. In the general case considered in this article, similar explicit expressions cannot be derived. Nevertheless, the equations introduced in the previous section can be conveniently solved in a sequential way. The aim of this section is to derive an explicit procedure to determine the boundaries of the complete separation region.

Let us first consider the strong components and reduce the corresponding mass balances to a simpler form. Eliminating y_i^E, y_i^{ES}, and θ_i^{ES} by substituting Eqs. 15 and 16 and using Eqs. 12 and 13, the mass balance (Eq. 17) reduces to:

$$\theta_i^2 - m_2 y_i^2 = (m_3 - m_2) y_i^F \quad (i \in E). \tag{23}$$

Similarly, for the weak components, using Eqs. 19 and 20, together with Eqs. 13 and 14, Eq. 21 gives:

$$m_3 y_i^3 - \theta_i^3 = (m_3 - m_2) y_i^F \quad (i \in R). \tag{24}$$

Equations 23 and 24 have a clear physical meaning. In particular, we note that the lefthand sides represent the absolute value of the quantities f_i^2 and f_i^3, respectively. Hence, Eq. 23 means that the net flow rate of each strong component in section 2 must be directed toward the extract outlet and must equal the entire flow rate of the same component fed to the unit, so that no fraction of it reaches the raffinate outlet. Similarly, Eq. 24 means that the net flow rate of each weak component in section 3 must be directed toward the raffinate outlet and must equal the entire flow rate of the same component fed to the unit, so that no fraction of its reaches the extract outlet. Thus, Eqs. 23 and 24 represent the requirement of complete separation.

To characterize the constant state in section 2 in terms of the operating parameters, we rewrite Eq. 23 using the equilibrium relationship (Eq. 5) and the definition of δ (Eq. 7):

$$y_i^2 (K_i - m_2 \delta_2) = \delta_2 (m_3 - m_2) y_i^F \quad (i \in E). \tag{25}$$

Since only the strong components and the desorbent can be present in section 2 (cf. Table 2), $\delta_2 = K_D y_D^2 + \Sigma_{i \in E} K_i y_i^2$. Using Eq. 25 to eliminate y_i^2, we obtain from the stoichiometric relationships, after some algebraic manipulations, the following relation:

$$1 - \frac{m_2 K_D}{m_2 \delta_2} = (m_3 - m_2) \sum_{i \in E} \frac{(K_i - K_D) y_i^F}{K_i - m_2 \delta_2}. \tag{26}$$

This is a $(NE+1)$ degree polynomial equation in the unknown $m_2\delta_2$, whose coefficients depend on the equilibrium constants, the feed composition, and the operating parameters, m_2 and m_3. Through Eq. 25, for given values of m_2 and m_3, its solution provides the composition of the constant state in section 2, y_i^2.

The constant state in section 3, y_i^3, can be characterized in a similar way, by first rewriting Eq. 24 as follows:

$$y_i^3 (m_3 \delta_3 - K_i) = \delta_3 (m_3 - m_2) y_i^F \quad (i \in R); \tag{27}$$

and then substituting in the stoichiometric relationships, which, upon noticing that $\delta_3 = K_D y_D^3 + \Sigma_{i \in R} K_i y_i^3$, lead to the following $(NR+1)$ degree polynomial equation in the unknown $m_3\delta_3$:

$$1 - \frac{m_3 K_D}{m_3 \delta_3} = (m_3 - m_2) \sum_{i \in R} \frac{(K_i - K_D) y_i^F}{m_3 \delta_3 - K_i}. \tag{28}$$

It may be noted that the states of the two central sections of the unit, represented by δ_2 and δ_3, respectively, appear separately in Eqs. 26 and 28, due to the enforced requirement of complete separation. The behavior of the two sections is connected only by the values of m_2 and m_3, which appear in both equations, thus confirming their tight interaction in determining the performance of the unit. Note also that neither m_1 nor m_4 is involved in these equations. Therefore, their choice does not influence the choice of m_2 and m_3, provided that m_1 and m_4 fulfill their relevant complete separation conditions in Table 2. On the other hand, Table 2 shows that m_1 in the case of strong desorbent and m_4 in the case of weak desorbent have bounds which depend on some of the Ω values, Ω_{NC-1}^{ES} and Ω_1^R, respectively, and thus on other m_j values. We will come back later to this case, since otherwise the constraints on m_1 and m_4 are explicit and do not require any further investigation.

The analytical solution of Eqs. 26 and 28, and then of the design problem itself, is worth pursuing only in the case where $NE = NR = 1$. This is the case of binary separations, which is considered in the next section. In all the other cases, it is convenient to solve Eqs. 26 and 28 numerically. Note that the search of the solutions of these equations can be limited to the interval $[K_{wk}, K_{sk}]$, due to the necessary conditions for complete separation given by Eqs. 8. The obtained solutions are used in the following procedure to determine whether the selected values of m_2 and m_3 allow to achieve complete separation or not.

1. The values of m_2 and m_3, which define a point in the $m_2 - m_3$ plane, are selected.
2. The solutions of Eqs. 26 and 28 are searched in the interval $[K_{wk}, K_{sk}]$. If one or both of these cannot be found, the procedure ends and we conclude that the point in the plane $m_2 - m_3$ under examination does not belong to the complete separation region. If one or both of Eqs. 26 and 28 have multiple solutions in the given interval, then the steps below must be repeated for all the possible solution pairs.
3. The composition of the constant states in sections 2 and 3 is calculated through Eqs. 25 and 27, respectively.
4. Through Eq. A2 in Appendix A, the corresponding Ω vectors are calculated. This leads to the determination of the Ω^γ vector corresponding to the state γ (Table 2), which allows to compute the composition of the state γ itself, y_i^γ and θ_i^γ.
5. Rewrite Eqs. 18 in terms of Ω parameters using the equilibrium theory relationships (Eqs. A6 and A7) in Appendix A. Since $\Omega_j^\beta = \Omega_j^\gamma$ for $j = 1, \ldots, NR$, Eqs. 18 constitute a system of NE equations in the NE unknowns $\Omega_{NR+1}^\beta, \ldots, \Omega_{NC-1}^\beta$. This system is solved numerically to obtain relevant Ω parameters.

6. Depending on the relative adsorptivity of the desorbent with respect to the species to be separated, the relevant conditions in Table 2 on the flow rates in sections 2 and 3 are checked.

Let us consider the projection on the $m_2 - m_3$ plane of the four-dimensional space of the operating parameters m_j for $j = 1, \ldots, 4$. We limit our analysis to the case where $m_3 > m_2 > -\epsilon_p/[\sigma(1-\epsilon_p)]$, which, following the definition of m_j and Eq. 13, is the only admissible one since it assumes that the fluid flow rates in sections 2 and 3, as well as in the feed stream, are positive. Following the procedure outlined above for all the points in this zone, we can determine the complete separation region in the $m_2 - m_3$ plane.

Each point in the region obtained above represents operating conditions for sections 2 and 3 which guarantee the achievement of complete separation, provided that the selected values of m_1 and m_4 satisfy the corresponding conditions in Table 2. These are independent of the values of m_2 and m_3 in the case of intermediate, weak-intermediate and strong-intermediate desorbent. However, the cases of weak and strong desorbent must be further analyzed with regard to the parameters m_4 and m_1, respectively.

In the case of weak desorbent, the upper bound for m_4 is given by Ω_1^R/K_D. Let us assume that the values of m_1, m_2 and m_3 fulfill the corresponding complete separation conditions: $m_1 > K_{NC}/K_D$, and m_2 and m_3 lie inside the complete separation region. To check whether a given value of m_4 fulfills the constraint above, we evaluate the composition of the state R through Eq. 19. Then, the corresponding Ω values are obtained using Eq. A2 and the specific value of Ω_1^R/K_D is compared with the given value of m_4. A similar procedure can be followed in the case of a strong desorbent to determine the value of Ω_{NC-1}^{ES}, which, when divided by K_D, determines the lower bound for m_1.

Application to Binary Mixtures: Role of the Desorbent Adsorptivity

In this section, we apply the general approach presented above to extend the results obtained for binary separations with intermediate desorbent in Part 1 to the case of binary separations with a desorbent having any adsorptivity value with respect to the two components to be separated.

A binary separation involves a three-component system: $NC = 3$. We adopt a more specific notation to identify the two chemical species in the feed stream: A for the most adsorbable component and B for the other.

The necessary and sufficient conditions to assure complete separation in the case of a binary feed can be easily derived from Table 2, where now only the cases of weak, intermediate and strong desorbent are possible. The parameter Ω_F characterizes the feed composition and is given through Eq. A2 in Appendix A by:

$$\Omega_F = \frac{K_A K_B}{K_A y_A^F + K_B y_B^F}. \tag{29}$$

Let us first consider the case of intermediate desorbent: $K_B < K_D < K_A$. Following the procedure outlined above, we consider Eq. 26, which in the case of a binary separation reduces to the quadratic equation:

$$(m_2\delta_2)^2 - (m_2\delta_2)[K_A + m_2 K_D - (K_A - K_D)(m_3 - m_2)y_A^F] + K_A K_D m_2 = 0. \tag{30}$$

Assume that the discriminant of this equation is positive and indicate the two roots as $\alpha^{\oplus}$ and $\alpha^{\ominus}$, with $\alpha^{\oplus} \geq \alpha^{\ominus}$. They satisfy the following relationship:

$$\alpha^{\oplus}\alpha^{\ominus} = K_A K_D m_2. \tag{31}$$

According to the above procedure, we should now repeat steps 3 through 6 for each one of the two roots. However, we can directly calculate Ω_2^{γ} by noting from Eq. A8 that in this case $\delta_2 = K_A K_D/\Omega_2^{\gamma}$, and then the two possible values for Ω_2^{γ} are $K_A K_D m_2/\alpha^{\oplus}$ and $K_A K_D m_2/\alpha^{\ominus}$. Thus, substituting Eq. 31 we obtain $\Omega_2^{\ominus} = \alpha^{\ominus}$ and $\Omega_2^{\oplus} = \alpha^{\oplus}$. Similarly, we can solve Eq. 28 in the unknown $(m_3\delta_3) = \beta$ leading to $\Omega_1^{\gamma\ominus} = \beta^{\ominus}$ and $\Omega_1^{\gamma\oplus} = \beta^{\oplus}$.

It is worth noting here that Eqs. 37 and 38 in Part 1, which contained the unknowns Ω_1^{γ} and Ω_2^{γ}, respectively, have the same coefficients as Eqs. 28 and 30 in the unknowns $(m_3\delta_3)$ and $(m_2\delta_2)$, respectively. This confirms the equality between the two pairs of roots of the equations obtained above. This result provides Ω_1^{γ} and Ω_2^{γ} in terms of m_3 and m_2, respectively. These can be substituted in the constraints on m_3 and m_2 in Table 2 to derive, following the procedure developed in Part 1, explicit expressions for the boundaries of the complete separation region in the $m_2 - m_3$ plane.

In the case of weak desorbent, $K_D < K_B < K_A$, the roots of Eqs. 26 and 28 correspond again to the values of Ω_2^{γ} and Ω_1^{γ}, respectively. We can then represent these parameters in terms of m_2 and m_3 and derive the expressions for the boundaries of the complete separation region in the $m_2 - m_3$ plane by

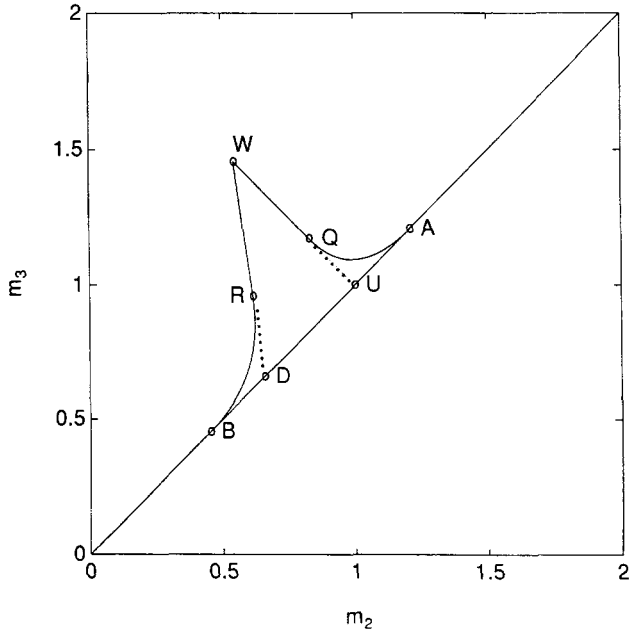

Figure 2. Region of complete separation in the $m_2 - m_3$ plane for an intermediate desorbent where $K_D > \Omega_F$.

$K_A = 2.67$, $K_B = 1$, $K_D = 2.21$, $y_A^F = 0.5$, $y_B^F = 0.5$, $\Omega_F = 1.46$ (Storti et al., 1989).

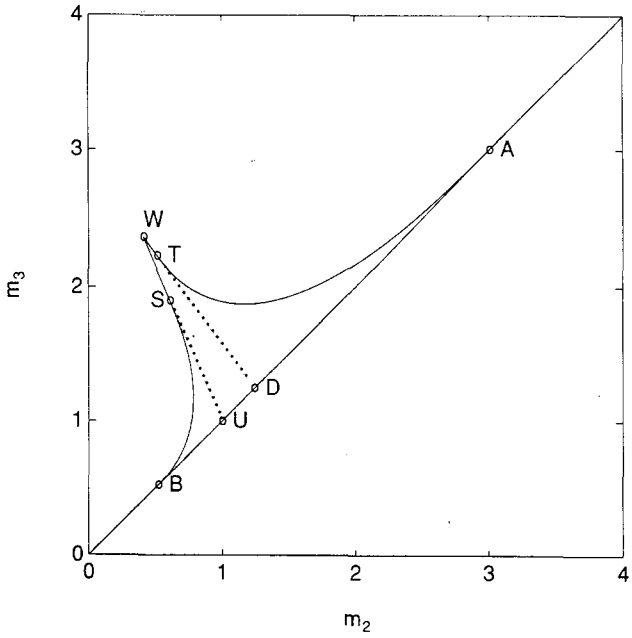

Figure 3. Region of complete separation in the $m_2 - m_3$ plane for an intermediate desorbent where $K_D < \Omega_F$.

$K_A = 5.71$, $K_B = 1$, $K_D = 1.9$, $y_A^F = 0.3$, $y_B^F = 0.7$, $\Omega_F = 2.37$ (Storti et al., 1989).

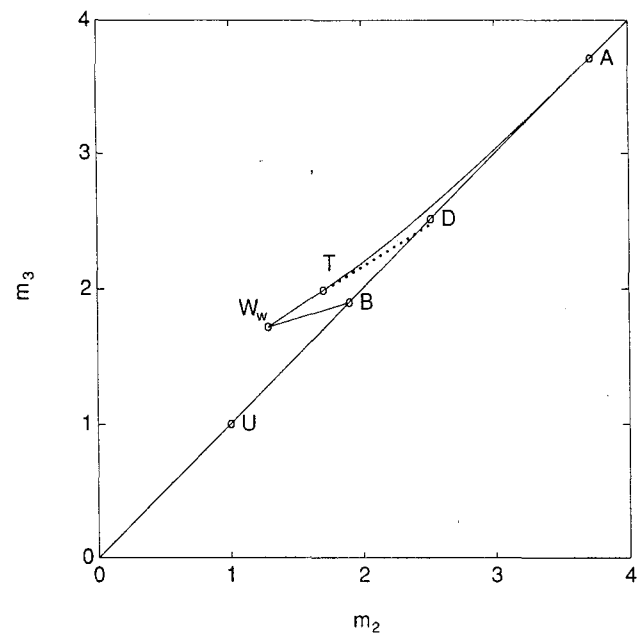

Figure 4. Region of complete separation in the $m_2 - m_3$ plane for weak desorbent.

$K_A = 5.71$, $K_B = 1.9$, $K_D = 1$, $y_A^F = 0.3$, $y_B^F = 0.7$, $\Omega_F = 2.37$.

following the same procedure adopted in Part 1. Similarly, we can treat the case of strong desorbent: $K_B < K_A < K_D$.

The complete separation region in the $m_2 - m_3$ plane in the case of intermediate desorbent is shown in Figures 2 and 3 for $K_D > \Omega_F$ and $K_D < \Omega_F$, respectively. In Figures 4 and 5 the complete separation region is shown in the case of weak and strong desorbent, respectively. The equations representing the boundaries of these regions are given in explicit form in the following, where proper reference to the relevant figures is made:

• Straight lines WD (Figures 2 and 3), W_wD (Figure 4) and W_sD (Figure 5):

$$K_A(K_D - K_B)m_2 + K_B(K_A - K_D)m_3 = \Omega_F(K_A - K_B) \quad (32)$$

• Straight line WU (Figures 2 and 3):

$$y_B^F m_2 + y_A^F m_3 = 1 \quad (33)$$

• Straight line W_wB (Figure 4):

$$[K_A(K_D - K_B) + K_B(K_A - K_D)y_B^F]m_2 + K_B(K_A - K_D)y_A^F m_3 = K_B(K_A - K_B) \quad (34)$$

• Straight line W_sA (Figure 5):

$$K_A(K_D - K_B)y_B^F m_2 + [K_A(K_D - K_B)y_A^F + K_B(K_A - K_D)]m_3 = K_A(K_A - K_B) \quad (35)$$

• Curves QA (Figure 2) and TA (Figures 3 and 4):

$$m_3 = m_2 + \frac{(\sqrt{K_A} - \sqrt{K_D m_2})^2}{y_A^F(K_A - K_D)} \quad (36)$$

• Curves RB (Figures 2 and 5) and SB (Figure 3):

$$m_2 = m_3 - \frac{(\sqrt{K_B} - \sqrt{K_D m_3})^2}{y_B^F(K_D - K_B)} \quad (37)$$

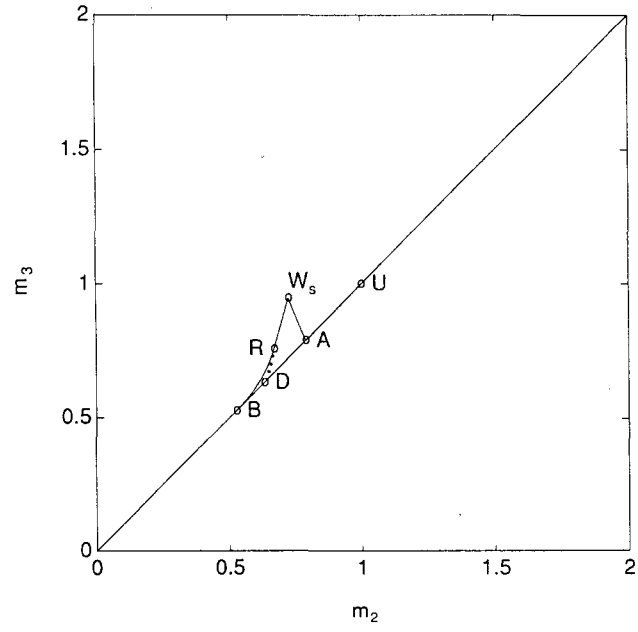

Figure 5. Region of complete separation in the $m_2 - m_3$ plane for strong desorbent.

$K_A = 1.5$, $K_B = 1$, $K_D = 1.9$, $y_A^F = 0.3$, $y_B^F = 0.7$, $\Omega_F = 2.37$.

• Straight line AB (Figures 2-5):

$$m_3 = m_2 \tag{38}$$

The coordinates of the intersection points are given by:

$$\text{point A} \quad \left(\frac{K_A}{K_D}, \frac{K_A}{K_D}\right) \tag{39}$$

$$\text{point B} \quad \left(\frac{K_B}{K_D}, \frac{K_B}{K_D}\right) \tag{40}$$

$$\text{point D} \quad \left(\frac{\Omega_F}{K_D}, \frac{\Omega_F}{K_D}\right) \tag{41}$$

$$\text{point U} \quad (1, 1) \tag{42}$$

$$\text{point Q} \quad \left(\frac{K_D}{K_A}, \frac{\Omega_F(K_A-K_B)-K_D(\Omega_F-K_B)}{K_B(K_A-\Omega_F)}\right) \tag{43}$$

$$\text{point R} \quad \left(\frac{\Omega_F[K_D(K_A-K_B)-\Omega_F(K_A-K_D)]}{K_AK_D(K_D-K_B)}, \frac{\Omega_F^2}{K_BK_D}\right) \tag{44}$$

$$\text{point S} \quad \left(\frac{\Omega_F(K_A-K_B)-K_D(K_A-\Omega_F)}{K_A(\Omega_F-K_B)}, \frac{K_D}{K_B}\right) \tag{45}$$

$$\text{point T} \quad \left(\frac{\Omega_F^2}{K_AK_D}, \frac{\Omega_F[K_D(K_A-K_B)-\Omega_F(K_D-K_B)]}{K_BK_D(K_A-K_D)}\right) \tag{46}$$

$$\text{point W} \quad \left(\frac{\Omega_F}{K_A}, \frac{\Omega_F}{K_B}\right) \tag{47}$$

$$\text{point W}_w \quad \left(\frac{K_B\Omega_F}{K_AK_D}, \frac{\Omega_F[K_D(K_A-K_B)+K_B(K_B-K_D)]}{K_BK_D(K_A-K_D)}\right) \tag{48}$$

$$\text{point W}_s \quad \left(\frac{\Omega_F[K_D(K_A-K_B)+K_A(K_D-K_A)]}{K_AK_D(K_D-K_B)}, \frac{\Omega_FK_A}{K_BK_D}\right) \tag{49}$$

The points inside the complete separation region in Figures 2-5 represent pairs of values for the operating parameters m_2 and m_3 which assure the achievement of complete separation, provided that the conditions on m_1 and m_4 in Table 2 are also satisfied.

Let us consider the case of weak desorbent, where the bound on m_1 is explicit: $m_1 > K_A/K_D$. On the contrary, the upper bound on m_4 is implicit and depends on m_2 and m_3 through Ω_1^R. By following the procedure described in the previous section, which in this case can be done analytically, the upper bound on m_4 reduces to $\Omega_1^{\ominus}/K_D$, where $\Omega_1^{\ominus}$ is the solution of Eq. 28. Similarly, in the case of strong desorbent the condition on m_4 is explicit, whereas that on m_1 reduces to $m_1 > \Omega_2^{\oplus}/K_D$, where $\Omega_2^{\oplus}$ is the solution of Eq. 26.

Figure 6 shows the complete separation regions for the same binary separation, that is, same values of K_A and K_B and same feed composition, but different values of the desorbent adsorptivity, K_D. This illustrates the effect of this parameter on

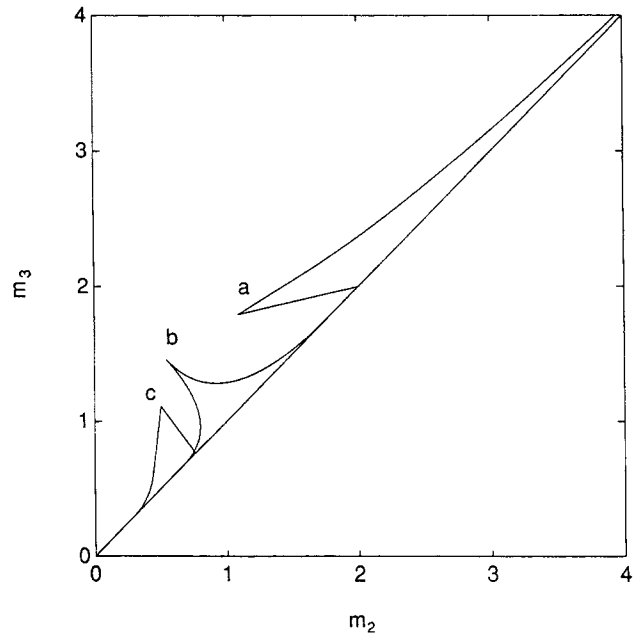

Figure 6. Effect of desorbent adsorptivity on the region of complete separation in the $m_2 - m_3$ plane.

$K_A = 2.67$, $K_B = 1$, $y_A^F = 0.5$, $y_B^F = 0.5$, $\Omega_F = 1.46$. (a) Weak desorbent: $K_D = 0.5$; (b) intermediate desorbent: $K_D = 1.5$; (c) strong desorbent: $K_D = 3.5$.

the shape and location of the complete separation region itself. It can be noted that in the case of intermediate desorbent the triangle-shaped region has a symmetric character with two tails, which are more or less stretched depending on the values of the adsorption selectivities and the feed composition.

In the other two cases only one tail is present. In the case of weak desorbent, higher values of m_2 and m_3 than in the case of intermediate desorbent are required to achieve complete separation for the same feed flow rate, that is, for the same value of the difference $(m_3 - m_2)$. On the contrary, lower values of m_2 and m_3 with respect to the case of intermediate desorbent are needed when the desorbent is strong.

Application to Multicomponent Mixtures

Results of the multicomponent theory

Using the procedure developed earlier, the region of complete separation of several multicomponent systems has been determined for illustrative purposes. In particular, we have considered three separations, each one of potential interest in applications, which represent three different situations with respect to the relative adsorptivity of the desorbent. These problems refer to the same mixture of the alkylaromatic C-8 fraction, with a typical industrial composition, but using different desorbent and adsorbent. The first and third cases in Figures 7 and 9 involve the separation of pure *p*-xylene from *m*-xylene, *o*-xylene and ethylbenzene using *p*-diethylbenzene as desorbent. In the two cases, however, two different adsorbents are considered, zeolites Sr-BaX and K-BaX, respectively, so that the relative adsorptivity of the involved components changes. As a consequence, in Figure 7 *p*-diethylbenzene is an intermediate desorbent, whereas in Figure 9 it is a strong desorbent. In Figure 8, we consider the separation of pure ethylbenzene from other components, using toluene

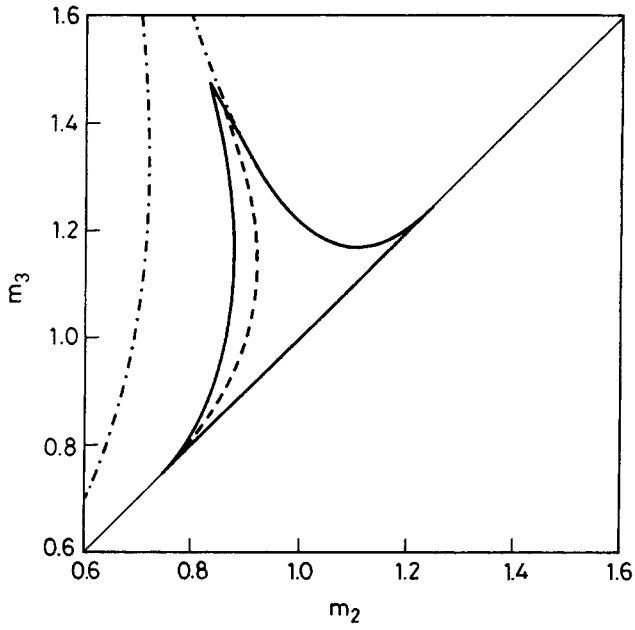

Figure 7. Region of complete separation in the $m_2 - m_3$ plane for a multicomponent system with intermediate desorbent.

Separation of *p*-xylene from *m*-xylene, *o*-xylene and ethylbenzene on Sr-BaX-zeolite, with *p*-diethylbenzene as desorbent (Ruthven, 1984). $K_{mX} = 1$, $K_{oX} = 1.18$, $K_{Eb} = 1.90$, $K_{pX} = 3.18$, $K_D = 2.56$; $y^F_{mX} = 0.4$, $y^F_{oX} = 0.1$, $y^F_{Eb} = 0.25$, $y^F_{pX} = 0.25$. —, exact complete separation region; - -, complete separation region for the pseudo-binary system defined by Eqs. 50–53; - • -, complete separation region for the pseudo-binary system defined by Eqs. 54 and 55.

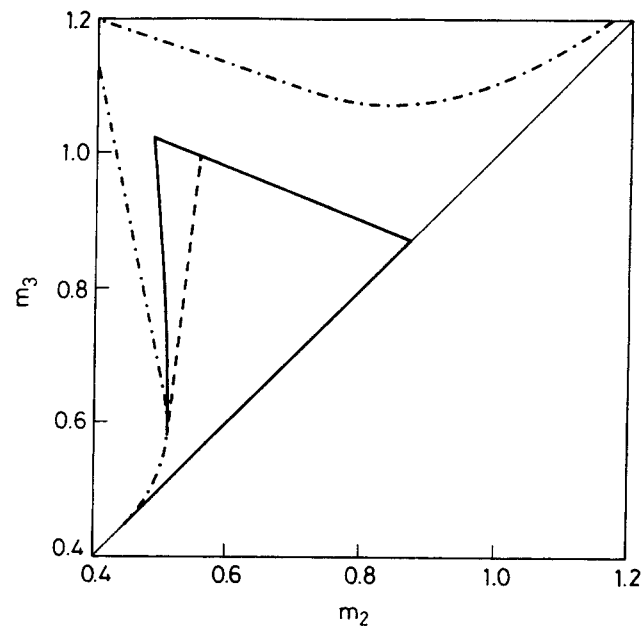

Figure 8. Region of complete separation in the $m_2 - m_3$ plane for a multicomponent system with strong-intermediate desorbent.

Separation of ethylbenzene from *m*-xylene, *o*-xylene and *p*-xylene on CaX-zeolite, with toluene as desorbent (Ruthven, 1984). $K_{Eb} = 1$, $K_{pX} = 1.98$, $K_{oX} = 2.59$, $K_{mX} = 3.11$, $K_D = 2.27$; $y^F_{Eb} = 0.25$, $y^F_{pX} = 0.25$, $y^F_{oX} = 0.1$, $y^F_{mX} = 0.4$. —, exact complete separation region; - -, complete separation region for the pseudo-binary system defined by Eqs. 50–53; - • -, complete separation region for the pseudo-binary system defined by Eqs. 54 and 55.

as desorbent and zeolite Ca-X as adsorbent. In this case, toluene is a strong intermediate desorbent.

Note that these three cases provide a rather interesting instance of application of the theoretical results obtained above, since the three possible relative adsorptivities of the desorbent are accounted for: intermediate, strong-intermediate, and strong. The adsorption equilibrium data for each system, taken from Table 12.6 of Ruthven (1984), are summarized in the caption of each figure, together with the relevant feed composition.

The regions of complete separation in Figures 7, 8, and 9 show that the parameters m_2 and m_3 are tightly interrelated, contrary to the case of a system described by a linear adsorption isotherm, where the boundaries of m_2 and m_3 are independent of each other. Moreover, the region of complete separation changes when the composition of the mixture to be separated changes. For example, the first case in Figure 10 shows that the region of complete separation becomes wider as the fraction of *p*-xylene, the desired component, in the feed stream increases.

In general, we observe that the shape of the region of complete separation in the $m_2 - m_3$ plane exhibits the same shape as that of the binary case. Thus, we can easily determine a region of robust operating conditions which guarantee the achievement of complete separation. By robust conditions we mean that small perturbations in the operating parameters do not modify the qualitative behavior of the unit. The procedure for selecting optimal and robust operating conditions in the case of multicomponent separation follows the same arguments described in Part 1 for binary separations. (Part I evaluates in detail the effect of disturbances in the operating conditions on the flow rate ratios m_j and then of the robust complete separation region.)

Shortcut approach

The theoretical analysis developed above provides the exact region of complete separation for a multicomponent system with any value of the desorbent adsorptivity in a four-section countercurrent unit. We have seen that for mixtures involving more than two components it is not possible to obtain an explicit analytical representation of the boundaries of the complete separation region. This is because in this case the roots of two generic polynomial equations, Eqs. 26 and 28, must be computed.

Analytical expressions for the boundaries of the complete separation region are rather useful, particularly at the earlier stages of the design of the separation unit. It is therefore attractive to develop an approximate shortcut method which allows one to treat the multicomponent case using explicit expressions.

To this aim, we reduce the multicomponent mixture to an equivalent pseudo-binary mixture constituted only of the weak-key and the strong-key components. The concentration of each of these in the feed stream is taken equal to the sum of the concentrations of all the weak and the strong components, respectively. Thus, the parameters of the pseudo-binary separation are given as a function of the corresponding parameters of the original multicomponent system by:

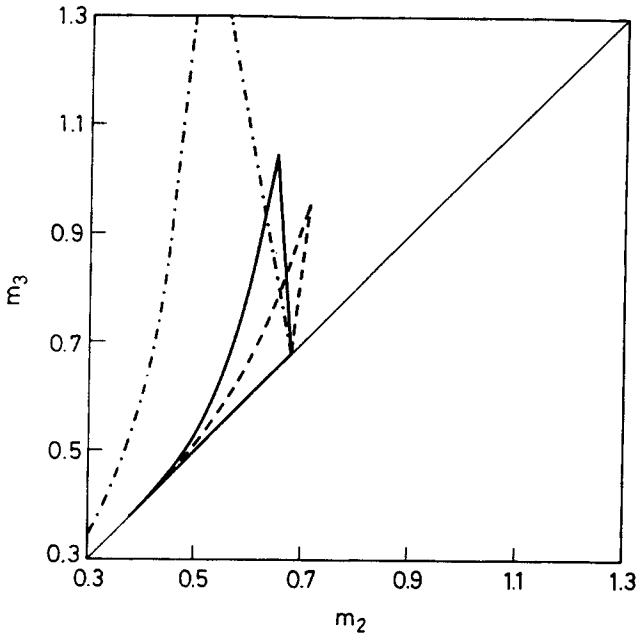

Figure 9. Region of complete separation in the $m_2 - m_3$ plane for a multicomponent system with strong desorbent.

Separation of *p*-xylene from *m*-xylene, *o*-xylene and ethylbenzene on K-BaX-zeolite, with *p*-diethylbenzene as desorbent (Ruthven, 1984). $K_{mX}=1$, $K_{oX}=1.11$, $K_{Eb}=2.33$, $K_{pX}=3.78$, $K_D=5.56$; $y^F_{mX}=0.4$, $y^F_{oX}=0.1$, $y^F_{Eb}=0.25$, $y^F_{pX}=0.25$. —, exact complete separation region; - -, complete separation region for the pseudo-binary system defined by Eqs. 50-53; - • -, complete separation region for the pseudo-binary system defined by Eqs. 54 and 55.

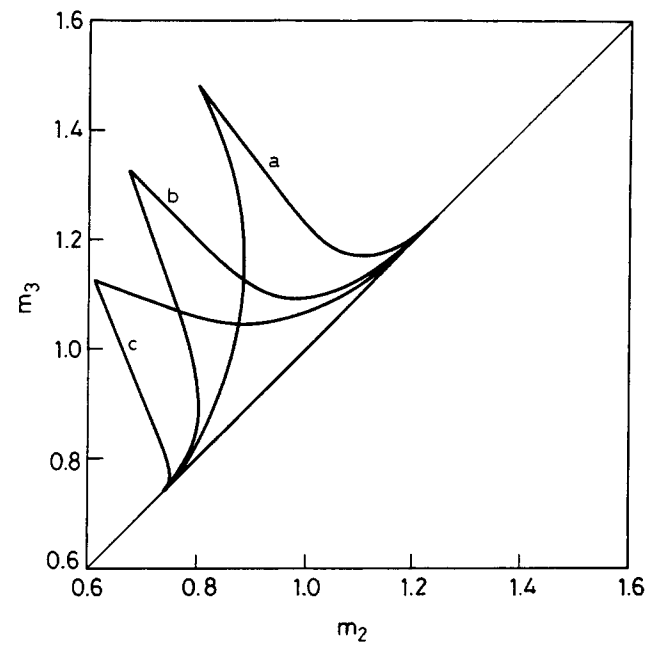

Figure 10. Effect of feed composition on the region of complete separation in the $m_2 - m_3$ plane.

Separation of *p*-xylene from *m*-xylene, *o*-xylene and ethylbenzene on Sr-BaX-zeolite, with paradiethylbenzene as desorbent (Ruthven, 1984). $K_{mX}=1$, $K_{oX}=1.18$, $K_{Eb}=1.90$, $K_{pX}=3.18$, $K_D=2.56$. (a) $y^F_{mX}=0.4$, $y^F_{oX}=0.1$, $y^F_{Eb}=0.25$, $y^F_{pX}=0.25$. (b) $y^F_{mX}=0.3$, $y^F_{oX}=0.05$, $y^F_{Eb}=0.15$, $y^F_{pX}=0.5$. (c) $y^F_{mX}=0.15$, $y^F_{oX}=0.05$, $y^F_{Eb}=0.05$, $y^F_{pX}=0.75$.

$$y^F_A=\sum_{i\in E} y^F_i, \tag{50}$$

$$y^F_B=\sum_{i\in R} y^F_i, \tag{51}$$

$$K_A=K_{sk}, \tag{52}$$

$$K_B=K_{wk}. \tag{53}$$

The desorbent adsorptivity K_D is the same as in the multicomponent case. Thus, the desorbent is intermediate in the pseudo-binary separation only if it is intermediate in the multicomponent separation. Similarly, it is either weak or strong in the pseudo-binary separation if it is either weak and weak intermediate or strong and strong-intermediate, respectively, in the multicomponent case. In all cases, the region of complete separation for the system defined by Eqs. 50 to 53 can be determined through the explicit relationships (Eqs. 32 to 38).

Note that using the definitions of K_A and K_B given by Eqs. 52 and 53, we obtain a binary system whose selectivity equals the smallest of the binary selectivities between the components to be collected in the extract and in the raffinate. Thus, $\min_{i\in E, j\in R}\{K_i/K_j\}=K_{sk}/K_{wk}$. Alternatively, we can consider a binary system whose selectivity equals the largest among the binary selectivities between the components in the extract and in the raffinate: $\max_{i\in E, j\in R}\{K_i/K_j\}=K_{ss}/K_{ww}$. Such a new pseudo-binary system is then characterized by

$$K_A=K_{ss} \tag{54}$$

$$K_B=K_{ww} \tag{55}$$

while the feed composition is again given by Eqs. 50 and 51. In this case, the desorbent is always intermediate, but when it is either strong or weak in the original multicomponent separation.

Let us analyze the relation between the multicomponent separation and each of the two pseudo-binary separations above by first considering the case of intermediate desorbent. Since the weak-key component is the most difficult to desorb among those to be collected in the raffinate, and the strong-key component is the most difficult to adsorb among those to be collected in the extract, the pseudo-binary separation defined by relations 50 to 53 is as difficult as, or in general more difficult than, the original multicomponent one. Therefore, the corresponding region of complete separation is supposed to be conservative with respect to the true one, a subset of the exact complete separation region of the original multicomponent separation. On the contrary, the region of complete separation of the multicomponent system is expected to be a subset of the region corresponding to the pseudo-binary separation defined by Eqs. 54 and 55. This is because in this case the binary separation involves the two components which are most likely to be collected in the extract and in the raffinate, components *ss* and *ww*, respectively. These properties are illustrated in Figure 7, where the exact complete separation region is compared with the regions obtained for the two pseudo-binary systems defined above.

In the case of weak-intermediate or strong-intermediate desorbent, the same conclusions about the relative position of the multicomponent and the pseudo-binary separation regions apply. The pseudo-binary separation defined by Eqs. 50 through 53 is in fact difficult, since in this case the desorbent is weak or strong, respectively. On the other hand, the binary separation defined by Eqs. 54 and 55 is much easier, since the desorbent is intermediate. These results are illustrated for the case of strong-intermediate desorbent in Figure 8.

Finally, a different picture occurs when a weak (or strong) desorbent is considered. In this case, for both pseudo-binary separations defined above the desorbent is weak (or strong). Therefore, the two separations are not easily related to each other as in the cases discussed above, but rather they are different, independent separations. This is shown in Figure 9, where the case of a strong desorbent is considered. It can be observed that the three complete separation regions are not contained one inside the other, but rather they intersect each other.

From the above analysis, we can conclude that, in all cases but in the case of weak or strong desorbent, the multicomponent complete separation region is enclosed between the corresponding regions of the two pseudo-binary separations defined by Eqs. 50 to 53 and Eqs. 54 and 55. This result is general enough for the separations of interest in the applications, since a weak or strong desorbent is in most cases not convenient (cf. Storti et al., 1989).

Let us now address the question of how close the multicomponent region of complete separation is approached by one or the other of the corresponding regions of the two pseudo-binary separations, in the cases of intermediate, weak-intermediate and strong-intermediate desorbent. In general, the answer depends on the specific composition of the multicomponent feed stream. However, the multicomponent region of complete separation is not very sensitive to changes in the composition of the feed stream.

This behavior is illustrated in Figure 11, where the separation of a four-component mixture is considered. Let us assume that the desired separation corresponds to collecting the two weakest species in the raffinate and the other two in the extract and that the desorbent is intermediate. The boundaries of the multicomponent complete separation regions in the figure are obtained by changing the feed composition, so that the overall concentration of weak and strong components remains unchanged. In this case, the two pseudo-binary separations defined above are not affected by the change in the feed composition, thus producing a unique region of complete separation each, as represented by the broken and the dotted lines (note that the broken line is hidden by the solid line c). While the feed composition changes, the exact region remains very close to the region corresponding to the pseudo-binary separation defined by Eqs. 50 to 53, at least for feed compositions including all four species.

Since this feature is general enough we can conclude that the region of complete separation for the pseudo-binary system (Eqs. 50 to 53) provides a good approximation of the true region for practical applications, in the cases of intermediate, weak-intermediate and strong-intermediate desorbent.

The above discussion applies to the operating parameters m_2 and m_3. A shortcut design procedure can be developed also for sections 1 and 4. We have already remarked that the bounds

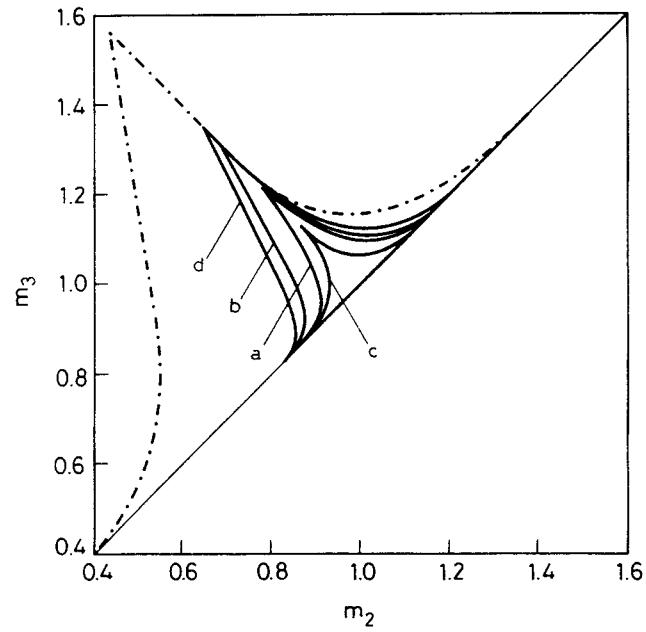

Figure 11. Assessment of the shortcut method.

Separation of ethylbenzene and *p*-xylene from *m*-xylene and *o*-xylene on CaX-zeolite, with toluene as desorbent (Ruthven, 1984). $K_{Eb}=1$, $K_{pX}=1.98$, $K_{oX}=2.59$, $K_{mX}=3.11$, $K_D=2.27$. —, exact complete separation region for different feed compositions; – –, complete separation region for the pseudo-binary system defined by Eqs. 50-53 (broken line is hidden by solid line c); - • -, complete separation region for the pseudo-binary system defined by Eqs. 54 and 55. (a) $y^F_{Eb}=0.25$, $y^F_{pX}=0.25$, $y^F_{oX}=0.1$, $y^F_{mX}=0.4$. (b) $y^F_{Eb}=0.45$, $y^F_{pX}=0.05$, $y^F_{oX}=0.05$, $y^F_{mX}=0.45$. (c) $y^F_{Eb}=0.05$, $y^F_{pX}=0.45$, $y^F_{oX}=0.45$, $y^F_{mX}=0.05$. (d) $y^F_{Eb}=0.49$, $y^F_{pX}=0.01$, $y^F_{oX}=0.01$, $y^F_{mX}=0.49$.

on m_1 and m_4 are not explicit only in the case of strong and weak desorbent, respectively. An approximate explicit bound on m_4 can be obtained by noting that, in the case of weak desorbent, if m_4 is chosen to be greater than 1, then the relevant condition in Table 2 is always fulfilled, since by definition $K_1=K_D\le\Omega_1^R\le K_2$. Correspondingly, in the case of strong desorbent, it is sufficient to choose $m_1>1$, since by definition $K_{NC-1}\le\Omega^{ES}_{NC-1}\le K_{NC}=K_D$, and therefore the relevant constraint on m_1 is satisfied.

To facilitate its application, the shortcut method has been summarized as a step-by-step procedure in Table 3.

Experimental Results

To compare the above theoretical results for a countercurrent unit, with the experimental performance of a simulated moving bed unit, we use the conversion rules between SMB and TCC units, based on their kinematic equivalence:

$$\frac{L}{t^*}=\frac{u_s}{1-\epsilon} \tag{56}$$

$$G_j=A\rho_f[u_j+u_s\epsilon/(1-\epsilon)]. \tag{57}$$

Thus, the flow rate ratio parameters m_j defined by Eq. 4 for TCC units, in the case of a SMB configuration, become:

$$m_j=\frac{G_jt^*-AL\epsilon^*\rho_f}{AL\rho_s\Gamma^\infty(1-\epsilon^*)}\quad(j=1,\ldots,4). \tag{58}$$

Table 3. Step-by-Step Procedure for the Shortcut Method

Step 1. Characterize the system to be separated with reference to the desorbent adsorptivity, from weak to strong, as described in Table 1.
- If the desorbent is either weak or strong, the shortcut procedure below cannot be applied and the numerical procedure in section 4 must be followed.
- If the desorbent is weak intermediate, intermediate, or strong intermediate, proceed with steps from 2 to 4.

Step 2. Determine the feed composition and equilibrium parameters of the equivalent pseudo-binary separation through Eqs. 50 to 53.

Step 3. The boundaries of the region of complete separation in the $m_2 - m_3$ plane for the pseudo-binary system can be calculated using different relations depending on the desorbent strength in the pseudo-binary separation. Three cases may arise:
- The desorbent is weak intermediate in the original multicomponent separation and then it becomes a weak desorbent in the pseudo-binary separation and Eqs. 32, 34, 36 and 38 must be used.
- The desorbent is intermediate in the original multicomponent separation, and then it remains intermediate in the pseudo-binary case and Eqs. 32, 33, 36, 37 and 38 must be used.
- The desorbent is strong-intermediate in the original multicomponent separation, and then it becomes a strong desorbent in the pseudo-binary separation and Eqs. 32, 35, 37 and 38 must be used.

Step 4. In all cases, the constraints for complete separation on the flow rate ratios m_3 and m_4 are explicit: $m_1 > K_{NC}/K_D$ and $-\epsilon_p/[\sigma(1-\epsilon_p)] < m_4 < K_1/K_D$.

The parameter m_j accounts for all the operating parameters typical of a SMB unit: the fluid flow rate G_j, the switching time t^*, the cross section A and length L of each column, and all the physical properties of the adsorbent.

Let us consider a set of experimental runs performed in a six-port simulated moving bed pilot plant operated in the vapor phase using a mixture of *m*-xylene, *p*-xylene and ethylbenzene, with isopropylbenzene as desorbent and KY-zeolite as adsorbent (Storti et al., 1992, 1993b). In Table 4 the relevant operating conditions and physicochemical data are summarized. Note that the components of the system under examination are ordered according to their increasing adsorptivity as follows: *m*-xylene, ethylbenzene, isopropylbenzene, and *p*-xylene.

Table 4. Physicochemical Data and Operating Conditions of Experimental Runs

Equilibrium Parameters	
Γ^{∞}	0.13 kg/kg
K_{mX}	1
K_{Eb}	1.34
K_D	1.50
K_{pX}	2.20
Operating temperature	523 K
Operating pressure	4×10^6 Pa
Feed composition	$y^F_{mX} = 0.499$, $y^F_{Eb} = 0.248$, $y^F_{pX} = 0.253$
ϵ	0.42
ϵ_p	0.21
ρ_s	1,490 kg/m^3
ρ_f	9.5 kg/m^3
A	1.767×10^{-4} m^2
L	1 m

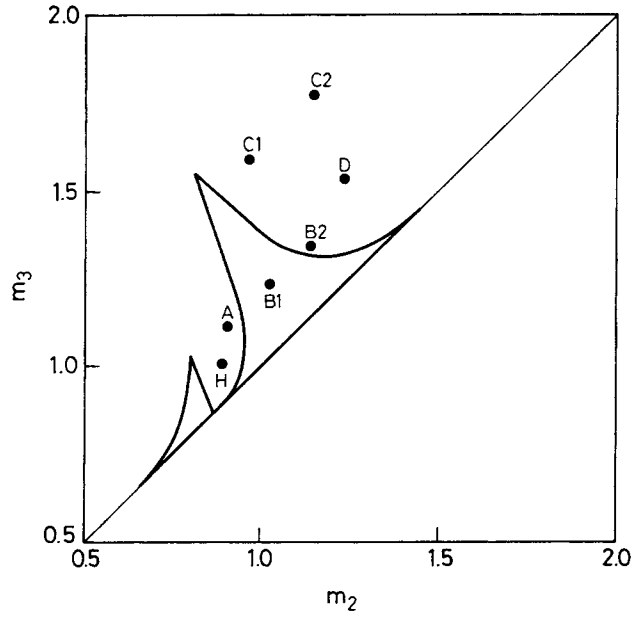

Figure 12. Comparison of the calculated multicomponent complete separation region in the $m_2 - m_3$ plane with experimental data (•) (Storti et al., 1993b).

Operating conditions, experimental and calculated separation performances are reported in Table 5. The region on the right-hand side refers to the problem of separating pure *p*-xylene in the extract; the region on the lefthand side refers to the problem of separating pure *m*-xylene in the raffinate.

Using the above three-component mixture, $NC = 4$, we consider two different separation problems. The first one requires that *p*-xylene alone is collected in the extract while leaving *m*-xylene and ethylbenzene in the raffinate. In the second, we recover *m*-xylene alone in the raffinate, while leaving *p*-xylene and ethylbenzene in the extract. With reference to the conventions adopted in the previous sections, in the first case the desorbent is intermediate and we have: $wk = 2$, $sk = 4$, $D = 3$, $NE = 1$, $NR = 2$. Moreover, set E consists of component 4, whereas set R of components 1 and 2. In the second case, the desorbent is a weak intermediate and $wk = 1$, $sk = 2$, $D = 3$, $NE = 2$, $NR = 1$. Set E includes components 2 and 4, whereas set R consists of component 1 alone.

Using the procedure developed earlier, we obtain two complete separation regions in the $m_2 - m_3$ plane, one for each of the separation problems considered. Obviously, the two regions are supposed to be disjoint. Moveover, since in the first case only *p*-xylene must be conveyed toward the extract outlet, values of the flow rates in sections 2 and 3, and consequently of the flow rate ratios m_2 and m_3, higher than those in the second case are expected. This is confirmed in Figure 12, where the predicted regions of complete separation corresponding to the first separation problem is on the righthand side, thus involving higher values of m_2 and m_3, whereas that one corresponding to the second separation problem is on the lefthand side, thus involving lower values of m_2 and m_3.

In Figure 12, the points representing the operating conditions adopted in the experimental runs aimed to obtaining *p*-xylene alone in the extract are reported. The values of the operating conditions of these experimental runs calculated through Eq. 58 are summarized in Table 5, together with the values of the

Table 5. Separation of *p*-Xylene from Ethylbenzene and *m*-Xylene: Operating Conditions and Performances of Experimental Runs

Run	Flow Rate Ratios				Purity Experimental		Purity Calculated	
	m_1	m_2	m_3	m_4	P_E (%)	P_R (%)	P_E (%)	P_R (%)
A	2.217	0.901	1.099	0.327	54.0	100	64.1	100
B1	2.217	1.019	1.219	0.321	96.7	100	100	100
B2	2.197	1.134	1.328	0.301	99.5	94.1	100	97.9
C1	2.198	0.966	1.604	0.307	98.0	87.2	100	90.6
C2	2.208	1.147	1.785	0.321	98.7	80.8	100	80.0
D	2.218	1.233	1.547	0.333	100	83.6	100	80.3
H	2.219	0.890	1.018	0.348	62.2	100	55.8	100

separation performances measured experimentally and calculated by the equilibrium theory model. As a measure of the process performance the following indexes are reported: purity in the extract stream, that is, the mole percentage of *p*-xylene in the extract with respect to the desorbent-free overall concentration, and purity in the raffinate stream, that is, the mole percentage of *m*-xylene and ethylbenzene in the raffinate with respect to the desorbent-free overall concentration. It can be seen that the quantitative agreement between experimental and calculated values is not always very close. This is mainly due to the assumption of constant selectivity in the adsorption equilibrium as well as to a slight deactivation of the zeolite which affected the separation performance in the last experimental runs.

Let us now consider the relative position of the points representing the experimental runs with respect to the predicted complete separation region in Figure 12. It appears that only the point corresponding to run B1 lies within the region of complete separation. Thus, we expect that only in this case complete separation conditions, 100% purity both in the extract and in the raffinate, should be achieved. This is confirmed by the experimental data in Table 5, where B1 is the experimental run which most closely approaches these conditions. However, we may note that the extract purity of 96.7% is too low. This is probably a consequence of the rather small size of the complete separation region in this specific example. The operating conditions corresponding to point B1 are rather close to the boundaries of this region, and this makes the corresponding separation performance very sensitive to uncertainties in the experimental parameters as well as to model errors.

Figure 12 also shows that the experimental runs corresponding to points located to the upper right of the complete separation region, B2, C1, C2, and D, fail to achieve complete separation conditions. In particlar they lead to purities very high in the extract and very low in the raffinate. On the other hand, the experimental runs corresponding to points located to the lower left of the complete separation region, A and H, also fail to achieve complete separation conditions, but in this case the purity values in the raffinate are very high, whereas those in the extract are very low.

These experimental findings are qualitatively in good agreement with the results of the equilibrium theory model in Table 5. It is worth mentioning that, as discussed in detail in Part 1 in the case of binary systems, this behavior is rather general. The region in the $m_2 - m_3$ plane located at the upper right of the complete separation region corresponds to operating conditions leading to pure extract (but not pure raffinate), while the region to the lower left corresponds to operating conditions leading to pure raffinate (but not pure extract).

Then, we can conclude that the coherence between the location of the experimental points with respect to the calculated complete separation region and the observed separation performance is satisfactory. This assesses the reliability and utility of the analysis developed in this work.

Concluding Remarks

The adsorption separation of multicomponent mixtures in a four-section countercurrent separation unit or in the equivalent simulated moving bed unit has been analyzed. In general, the design of their operating conditions to achieve the desired separation performance is rather difficult, because of their complex behavior.

In this article, which follows Part 1 on the same subject but limited to binary separations with a desorbent having an intermediate adsorptivity with respect to those of the species to be separated (Storti et al., 1993a), the analysis is developed in the frame of equilibrium theory. According to this approach, the adsorption equilibria are described through the constant selectivity stoichiometric model, whereas mass-transfer resistances and axial mixing are neglected. Nevertheless, this model describes the key features of the separation processes well.

By considering the general case of a multicomponent system with a desorbent having any adsorptivity, a region in the operating parameters space has been determined in terms of the adsorption equilibrium constants and the feed stream composition. The points inside this region represent operating conditions which achieve complete separation. In the case of linear adsorption equilibria, the complete separation region becomes independent of the desorbent adsorptivity and the feed composition.

The geometric representation of the complete separation region in the $m_2 - m_3$ plane allows to elucidate the role of the operating parameters in determining the separation performance. These are the fluid flow rates and the solid velocity in the case of a TCC unit and the fluid flow rates, the switching time and the port length in the case of a SMB unit. This result allows to predict the effect of increasing or decreasing the fluid flow rate in any section of the unit, as it has been confirmed by comparison with experimental results obtained in a six-port SMB unit operated in the vapor phase for the separation of a three-component mixture.

In the case of a binary mixture, the region of complete separation can be easily determined through explicit relationships that define its boundaries. In the general case of a multicomponent mixture, numerical techniques must be used. Thus, a shortcut approach has been proposed, which allows one to obtain an approximate region of complete separation using again explicit relationships. This is based on the concept of strong-key and weak-key components, which allows to reduce the multicomponent system to an equivalent binary system. It has been shown that the shortcut method produces a conservative, though rather close, approximation of the true region.

Acknowledgments

We gratefully acknowledge the financial support of CNR Progetto Finalizzato Chimica Fine II.

Notation

A = cross section of the adsorption column
C = equilibrium theory function, defined by Eq. B2
D = desorbent
E = set of strong components collected in the extract stream
f_i^j = dimensionless net flow rate of component i in section j, $f_i^j = m_j y_i^j - \theta_i^j$
F = equilibrium theory function, defined by Eq. B1
G_j = fluid mass-flow rate in section j of a SMB unit
K_i = equilibrium adsorption constant of component i
L_j = length of section j
m_j = mass-flow rate ratio in section j, defined by Eqs. 4 and 58
NC = total number of components
NE = number of strong components
NR = number of weak components
P_E = desorbent-free extract purity
P_R = desorbent-free raffinate purity
R = set of weak components collected in the raffinate stream
S = equilibrium theory function, defined by Eq. B3
t = time
t^* = switching time in a SMB unit
u_j = superficial fluid phase velocity in section j
u_s = superficial solid phase velocity
x = dimensionless axial coordinate, $x = z/L_j$
y_i^j = fluid phase dimensionless concentration of component i in section j
z = axial coordinate

Greek letters

α = root of Eq. 30
β = root of Eq. 28
Γ^∞ = adsorbed-phase saturation concentration
δ = equilibrium theory parameter, defined by Eq. 7
ϵ = external void fraction
ϵ_p = intraparticle void fraction
ϵ^* = overall void fraction, $\epsilon^* = \epsilon + \epsilon_p(1-\epsilon)$
θ_i^j = adsorbent coverage fraction of component i in section j
μ_j = volumetric flow rate ratio in section j, $\mu_j = u_s/u_j$
ρ_f = fluid phase density
ρ_s = bulk solid mass density
σ = capacity ratio, $\sigma = \rho_s\Gamma^\infty/\rho_f$
τ = dimensionless time, $\tau = tu_s/L$
Ω = equilibrium theory parameter defined by Eq. A2

Subscripts and superscripts

a = section a
A, B = components to be separated
b = section b
c = constant state in the column
cs = complete separation
D = desorbent
E = extract
f = fluid state
F = feed
i = component index
j = section index
k = constant state index
l = component index
o = initial condition
p = outgoing state, after mixing
R = raffinate
s, S = solid state
sk = strong-key component
ss = strongest component in the mixture to be separated
wk = weak-key component
ww = weakest component in the mixture to be separated
α, β, γ = streams in the four-section separation unit, defined in Figure 1
$\oplus, \ominus$ = greatest and smallest root of a quadratic equation, respectively

Literature Cited

Broughton, D. B., and C. G. Gerhold, "Continuous Sorption Process Employing Fixed Beds of Sorbent and Moving Inlets and Outlets," U.S. Patent 2,985,589 (May 23, 1961).

Ganetsos, G., and P. E. Barker, "Semicontinuous Countercurrent Chromatographic Refiners," *Preparative and Production Scale Chromatography*, G. Ganetsos and P. E. Barker, eds., Marcel Dekker, New York (1993).

Hashimoto, K., S. Adachi, Y. Shirai, and M. Morishita, "Operation and Design of Simulated Moving-Bed Adsorbers," *Preparative and Production Scale Chromatography*, G. Ganetsos and P. E. Barker, eds., Marcel Dekker, New York (1993).

Helfferich, F. G., "The h- and ω-Transformations in Multicomponent Fixed-Bed Ion Exchange and Adsorption: Equivalent Mathematics, Different Scope," *Chem. Eng. Sci.*, **46**, 3320 (1991).

Helfferich, F., and G. Klein, *Multicomponent Chromatography: Theory of Interference*, Marcel Dekker, New York (1970).

Johnson, J. A., and R. G. Kabza, "SORBEX: Industrial-Scale Adsorptive Separation," *Preparative and Production Scale Chromatography*, G. Ganetsos and P. E. Barker, eds., Marcel Dekker, New York (1993).

Paludetto, R., G. Gamba, G. Storti, S. Carrà, and M. Morbidelli, "Multicomponent Adsorption Equilibria of Highly Non-Ideal Mixtures: the Case of Chloroaromatic Mixtures on Zeolite," *Chem. Eng. Sci.*, **42**, 2713 (1987a).

Paludetto, R., G. Storti, G. Gamba, S. Carrà, and M. Morbidelli, "On Multicomponent Adsorption Equilibria of Xylene Mixtures on Zeolites," *I&EC Res.*, **26**, 2250 (1987b).

Rhee, H.-K., R. Aris, and N. Amundson, "Multicomponent Adsorption in Continuous Countercurrent Exchangers," *Phil. Trans. Roy. Soc. London*, **A269**, 187 (1971).

Rhee, H.-K., R. Aris, and N. Amundson, *First-Order Partial Differential Equations*, Vol. II, Prentice-Hall, Englewood Cliffs, NJ (1989).

Ruthven, D. M., *Principles of Adsorption and Adsorption Processes*, Wiley, New York (1984).

Ruthven, D. M., and C. B. Ching, "Counter-Current and Simulated Counter-Current Adsorption Separation Processes," *Chem. Eng. Sci.*, **44**, 1011 (1989).

Storti, G., M. Masi, S. Carrà, and M. Morbidelli, "Optimal Design of Multicomponent Adsorption Separation Processes Involving Nonlinear Equilibria," *Chem. Eng. Sci.*, **44**, 1329 (1989).

Storti, G., M. Mazzotti, L. T. Furlan, M. Morbidelli, and S. Carrà, "Performance of a Six Port Simulated Moving Bed Pilot Plant for Vapor-Phase Adsorption Separation," *Sep. Sci. & Technol.*, **27**, 1889 (1992).

Storti, G., M. Mazzotti, M. Morbidelli, and S. Carrà, "Robust Design of Binary Countercurrent Adsorption Separation Processes," *AIChE J.*, **39**, 471 (1993a).

Storti, G., M. Mazzotti, L. T. Furlan, and M. Morbidelli, "Analysis of a Six Port Simulated Moving Bed Separation Unit," *Fundamentals of Adsorption*, M. Suzuki, ed., Kodansha, Tokyo, p. 607 (1993b).

Appendix A

The main results of equilibrium theory in the case of a single countercurrent column, which are relevant to this work, are summarized. Note that we adopt the approach based on the ω transformation (cf. Rhee et al., 1989; Storti et al., 1989, 1993a) rather than the equivalent one based on the h transformation (cf. Helfferich and Klein, 1970; Helfferich, 1991). Let us consider a NC-component system characterized by the constant selectivity stoichiometric equilibrium model:

$$\theta_i = \frac{K_i y_i}{\sum_{j=1}^{NC} K_j y_j} \quad (i = 1, \ldots, NC). \tag{A1}$$

Through equilibrium theory, there exists a one-to-one mapping between the space of fluid or adsorbed-phase concentra-

tions and a $(NC-1)$-dimensional Ω space, whose components are obtained as roots of the equation:

$$\sum_{i=1}^{NC} \frac{K_i y_i}{K_i - \Omega} = 0, \tag{A2}$$

or

$$\sum_{i=1}^{NC} \frac{\theta_i}{K_i - \Omega} \triangleq 0. \tag{A3}$$

Moreover, the Ω parameters are roots of the equation:

$$\sum_{i=1}^{NC} \frac{K_i \theta_i}{K_i - \Omega} = 1, \tag{A4}$$

and fulfill the following inequalities:

$$K_1 \le \Omega_1 \le K_2 \le \ldots \le K_i \le \Omega_i \le K_{i+1} \le \ldots \le K_{NC-1} \le \Omega_{NC-1} \le K_{NC}, \tag{A5}$$

where $\Omega = K_i$ if and only if $y_i = \theta_i = 0$. Equations A2 and A3 can be inverted leading for $i = 1, \ldots, NC$ to:

$$\theta_i = \left(\prod_{j=1}^{NC-1} (K_i - \Omega_j) \right) \Big/ \left(\prod_{j=1, j\neq i}^{NC} (K_i - K_j) \right), \tag{A6}$$

$$y_i = \theta_i \left(\prod_{j=1, j\neq i}^{NC} K_j \right) \Big/ \left(\prod_{j=1}^{NC-1} \Omega_j \right). \tag{A7}$$

Let us define $\delta = \Sigma_{j=1}^{NC} K_j y_j$, hence $\theta_i = K_i y_i / \delta$. It follows from Eqs. A1 and A7 that:

$$\delta = \left(\prod_{j=1}^{NC} K_j \right) \Big/ \left(\prod_{j=1}^{NC-1} \Omega_j \right). \tag{A8}$$

Let us now consider the generic section of the countercurrent unit in Figure 1 and the two incoming states corresponding to the vectors Ω^a (the fluid state) and Ω^b (the adsorbed state). At steady-state conditions, the fluid and adsorbed phases have constant composition in the entire column. Its specific composition is determined by the value of the net flow rate ratio m, and the corresponding Ω^c vector can take one of the following general configurations:

$$\Omega^c = (\Omega_1^a, \ldots, \Omega_k^a, \Omega_{k+1}^b, \ldots, \Omega_{NC-1}^b), \tag{A9}$$

where k can take any of the integer values between 0 and $NC-1$. The choice of k depends on the value of the mass-flow rate ratio m. The conditions for the occurrence of one particular constant state can be expressed in terms of the product of m with the quantity δ, which refers to the constant state inside the column: it is calculated through Eq. A8 using the Ω values in Eq. A9 for the particular value of k considered. In particular, each constant state of kind k is associated with a particular interval of values of the product $m\delta$, according to the following rules:

$$\frac{-\epsilon_p \delta}{\sigma(1-\epsilon_p)} \le m\delta \le \min\{\Omega_1^a, \Omega_1^b\}, \quad k = 0, \tag{A10}$$

$$\max\{\Omega_k^a, \Omega_k^b\} \le m\delta \le \min\{\Omega_{k+1}^a, \Omega_{k+1}^b\}, \quad k = 1, \ldots, NC-2, \tag{A11}$$

$$\max\{\Omega_{NC-1}^a, \Omega_{NC-1}^b\} \le m\delta < +\infty, \quad k = NC-1. \tag{A12}$$

In the case where $\Omega_k^b < \Omega_k^a$ for some $k = 1, \ldots, NC-1$, then the constant state can correspond also to the vector:

$$\Omega^c = (\Omega_1^a, \ldots, \Omega_{k-1}^a, \Omega_k, \Omega_{k+1}^b, \ldots, \Omega_{NC-1}^b), \tag{A13}$$

with $\Omega_k^b < \Omega_k < \Omega_k^a$ and $m\delta = \Omega_k$. We do not consider this case here, because it is not relevant to determining the complete separation region, as it was demonstrated in the case of binary separations in Appendix C of Part 1.

Appendix B

We prove here the complete separation proposition stated in Theorem 1. The importance of this proposition stems from the fact that in each section of the unit a constant state of only one kind identified by only one specific value of the index k (see Eq. A9) is compatible with the requirement of complete separation. It follows that only one configuration of the unit is consistent with such a requirement and that every operating parameter $m_j, j = 1, \ldots, 4$, is constrained to belong to a unique interval.

Note that the constraint given by Eq. 10 on Ω_i values in the unit has been demonstrated in Part 1, Theorem 2.

The starting point for the proof of the complete separation proposition is the necessary condition for complete separation given by Eqs. 8. They are conditions on the quantities $m_j\delta_j$, which must belong to intervals bounded by values of the equilibrium constants. Now, it is necessary to verify for each section of the unit which steady constant state, that is, which index k, is compatible with these necessary conditions. In the frame of equilibrium theory, every different state of each section j can be selected by the value of the mass-flow rate ratio m_j, properly chosen so that the quantity $m_j\delta_j$ is within a different range of values, given by Eqs. A10 to A12. To prove the complete separation proposition for each section of the unit, first the intersection set between the conditions given by Eqs. 8 and those given by Eqs. A10 to A12 must be found, and then it must be checked that all the values of $m_j\delta_j$ within the obtained set are compatible with the behavior of the neighboring sections of the unit.

In the following we are not considering the case where at steady state one of the states across a simple wave prevails within a section of the unit. In fact, in Part 1, Appendix C, it was proved that even though this case can produce a set of complete separation operating conditions they correspond to points on the boundary of the complete separation region, not internal points, hence they have no interest for applications. The same property can be easily extended to the general case of multicomponent separation.

Section 1

From Eqs. 8 the necessary condition is $K_{ss} < m_1\delta_1 < +\infty$. This

interval must be compared with the range of $m_1\delta_1$ corresponding to the state $(NC-1)$ given by Eq. A12. In this case, $\Omega^a_{NC-1}=K_{ss}$ because the fluid stream must be pure desorbent, whereas $\Omega^b_{NC-1}=\Omega^{ES}_{NC-1}$, which by definition is a value between K_{NC-1} and K_{NC}. If the desorbent is not strong, then $ss=NC$, $\max\{\Omega^a_{NC-1}, \Omega^b_{NC-1}\}=K_{NC}$ and the range given by Eq. A12 coincides with the above necessary condition. On the contrary, if the desorbent is strong, then $ss=NC-1$ and $\max\{\Omega^a_{NC-1}, \Omega^b_{NC-1}\}=\Omega^{ES}_{NC-1}$, thus the necessary and sufficient condition for complete separation is $\Omega^{ES}_{NC-1}<m_1\delta_1<+\infty$. Since in both cases at steady state the fluid states prevail within the section, $\delta_1=K_D$ and the constraints in Table 2 are obtained.

Section 4

Necessary and sufficient conditions for section 4 are obtained following the same arguments as for section 1.

Section 2

First, let us consider the case of intermediate desorbent: $K_{wk}<K_D<K_{sk}$ and $D=wk+1=sk-1=NR+1$. From Eqs. 8, the necessary conditions for complete separation impose that $m_2\delta_2$ belongs to an interval that we call I_{cs}: $I_{cs}=(K_{wk}, K_{sk})$.

The first NR values of Ω parameters corresponding to the incoming fluid state are the equilibrium constants $K_1, \ldots, K_{wk}$ (see Table 2). It follows that: $\max\{\Omega^a_{wk-1}, \Omega^b_{wk-1}\}=\Omega^\gamma_{wk-1}<K_{wk}$; $\min\{\Omega^a_{wk}, \Omega^b_{wk}\}=K_{wk}$; $\max\{\Omega^a_{wk}, \Omega^b_{wk}\}=\Omega^\gamma_{wk}>K_{wk}$; $K_D<\Omega^a_{wk+1}, \Omega^b_{wk+1}<K_{sk}$; $\min\{\Omega^a_{sk}, \Omega^b_{sk}\}>K_{sk}$. If we call I_k the range of $(m_2\delta_2)$ values given by Eqs. A10 to A12 corresponding to the kth constant state, the following relationships hold true: $I_{wk-1}=(\Omega^\gamma_{wk-1}, K_{wk})\cap I_{cs}=\emptyset$; $I_{wk}=(\Omega^\gamma_{wk}, \min\{\Omega^E_{wk+1}, \Omega^\gamma_{wk+1}\})\subset I_{cs}$; $I_{wk-1}\cap I_{cs}=\emptyset$; $I_{wk}\subset I_{cs}$; $I_{wk+1}\cap I_{cs}\neq\emptyset$. Therefore, the state wk is acceptable, whereas the state $(wk+1)$ must be discarded.

Let us identify the fluid stream with the superscript f, the solid stream with s and the constant state inside the column with c, and let $F(\Omega)$, $C(\Omega)$ and $S(\Omega)$ be the functions whose zeroes are the Ω values characterizing the fluid, constant and solid states respectively:

$$F(\Omega)=\sum_{i=1}^{NC}\frac{K_i y_i^f}{K_i-\Omega}, \tag{B1}$$

$$C(\Omega)=\sum_{i=1}^{NC}\frac{\theta_i^c}{K_i-\Omega}, \tag{B2}$$

$$S(\Omega)=\sum_{i=1}^{NC}\frac{K_i y_i^s}{K_i-\Omega}. \tag{B3}$$

From Eq. 99 of Part 1, Appendix A, the following equation can be derived:

$$\frac{F(\Omega)}{\mu(1-\epsilon_p)\sigma}=(m\delta^c-\Omega)C(\Omega)+\left(\Omega\delta^s+\frac{\epsilon_p}{(1-\epsilon_p)\sigma}\right)S(\Omega). \tag{B4}$$

If the state $(wk+1)$ prevailed in section 2, then the $(NR+1)$th Ω value of the steady constant state inside the column would equal Ω^E_{NR+1}. From the second part of Theorem 1, Part 1, it follows that also $\Omega^{ES}_{NR+1}=\Omega^E_{NR+1}$. Under this assumption, let us set $\Omega=\Omega^E_{NR+1}$ in Eq. B4 and note that $F(\Omega^E_{NR+1})=S(\Omega^E_{NR+1})=0$. It follows that $(m_1\delta_1-\Omega^E_{NR+1})C(\Omega^E_{NR+1})=0$. We have already shown that the steady constant state inside section 1 is pure desorbent, hence $C(\Omega^E_{NR+1})\neq 0$ and $m_1\delta_1$ must equal Ω^E_{NR+1}. But this contradicts the requirement that $m_1\delta_1>K_{NC}$, since by definition $\Omega^E_{NR+1}\leq K_{NR+2}=K_{sk}\leq K_{NC}$.

Thus, it has been demonstrated that if the desorbent is intermediate the only steady constant state in section 2 compatible with the requirement of complete separation is the state wk. The range of values of $m_2\delta_2$ has Ω^γ_{wk} as lower bound and $\min\{\Omega^E_{wk+1}, \Omega^\gamma_{wk+1}\}$ as upper bound.

The upper bound can be defined more precisely, since it can be proved that it always equals Ω^γ_{wk+1}. For this, let us consider Ω vectors associated to the steady constant states in sections 1 and 2. If the desorbent is intermediate $\Omega^1_i=\Omega^2_i$ for $i=1, \ldots, NR$ and $\Omega^1_i=K_{i+1}>\Omega^2_i=\Omega^\gamma_i$ for $i=NR+1, \ldots, NC-1$. It follows that $\delta_2>\delta_1$ and therefore, since $m_1>K_{NC}/\delta_1\geq K_i/\delta_1$, we also have that $m_1>K_i/\delta_1>K_i/\delta_2$. Now, if the righthand side of Eq. 15 is substituted into Eq. 23, the following equation is obtained after a proper rearrangement:

$$y_i^2(K_i/\delta_2-m_2)=(m_1-m_2)y_i^E \quad \forall i\in E. \tag{B5}$$

From the above inequality, it follows that $y_i^E<y_i^2$, $\forall i\in E$; as a consequence, $y_D^E>y_D^2$, because only the strong components and the desorbent are present in these streams. We can now apply this result to show that $\Omega^E_{wk+1}>\Omega^\gamma_{wk+1}$.

Both Ω^E_{wk+1} and Ω^γ_{wk+1} are greater than K_D, since by definition $\Omega_{wk+1}>K_{wk+1}$ and by assumption $D=wk+1$. Moreover, they are lower than K_i, $\forall i\in E$. For both states, the state inside section 2 and the extract stream, Ω values are the roots of Eq. A2, which can now be written as:

$$\sum_{i\in E}\frac{K_i y_i}{K_i-\Omega}=\frac{K_D y_D}{\Omega-K_D}. \tag{B6}$$

Since $\Omega^2_{wk+1}=\Omega^\gamma_{wk+1}$, it follows that:

$$\sum_{i\in E}\frac{K_i y_i^2}{K_i-\Omega^\gamma_{wk+1}}=\frac{K_D y_D^2}{\Omega^\gamma_{wk+1}-K_D}. \tag{B7}$$

On the contrary, from the above inequalities and since each term in the sum of the preceding equation is positive, we obtain that:

$$\sum_{i\in E}\frac{K_i y_i^E}{K_i-\Omega^\gamma_{wk+1}}<\frac{K_D y_D^E}{\Omega^\gamma_{wk+1}-K_D}. \tag{B8}$$

Since the lefthand side of Eq. B6 is an increasing function of Ω in the interval (K_{wk+1}, K_{wk+2}) and the righthand side is a decreasing function of Ω in the same interval, it follows that $\Omega^E_{wk+1}>\Omega^\gamma_{wk+1}$.

This concludes the proof of the necessary and sufficient conditions for complete separation in the case of intermediate desorbent.

Let us now consider the case of weak and weak-intermediate desorbent: $K_D<K_{wk}$, $D<wk=NR+1=sk-1$. In this case, if in the Ω vector associated to the extract stream a Ω value different from an equilibrium constant were present among the values corresponding to the equilibrium constants of the

weak components, that is, if $\exists\Omega_j^E$ such that $\Omega_j^E < K_{wk}$, then this would not contradict the fundamental inequalities (Eq. A6) on the values of Ω parameters. However, this cannot happen, because in this case also $\Omega_j^{ES} = \Omega_j^E$; as in the previous case of the $(wk+1)$ state, $m_1\delta_1 = \Omega_j^E < K_{NC}$, which violates the constraint on the parameter m_1. Therefore, in the case of weak or weak-intermediate desorbent the Ω vector associated to the extract stream is the same as in the case of any other desorbent adsorptivity.

In this case, $\max\{\Omega_{wk-1}^a, \Omega_{wk-1}^b\} = K_{wk}$; $K_{wk} < \Omega_{wk}^a$, $\Omega_{wk}^b < K_{sk}$; $K_{sk} < \min\{\Omega_{wk+1}^a, \Omega_{wk+1}^b\}$. An analogous derivation, as the one developed above through Eqs. B5 to B8, demonstrates that $\Omega_{wk}^\gamma < \Omega_{wk}^E$. It is worth noting that if the mentioned equations were written in terms of the parameter NR instead of wk, they would apply to all the cases of different desorbent absorptivity, that is, intermediate, weak-intermediate, and weak, provided that the proper relationship between NR and wk is used (see Table 2). It follows that: $I_{wk-1} = (K_{wk}, \Omega_{wk}^\gamma) \subset I_{cs}$ and $I_{wk} = (\Omega_{wk}^E, \min\{\Omega_{wk+1}^a, \Omega_{wk+1}^b\}) \cap I_{cs} \neq \emptyset$.

By following the same argument used above to discard the state $(wk+1)$ in the case of intermediate desorbent, we can now discard the state wk. Therefore, the only steady constant state which is compatible in section 2 with complete separation is the state $(wk-1)$, that is, the state NR, with the bounds reported in Table 2.

Now, we can conclude for the case of strong and strong-intermediate desorbent that: $K_D > K_{sk}$, $D > sk = NR+1 = wk+1$. In this case, $\max\{\Omega_{wk-1}^a, \Omega_{wk-1}^b\} = \Omega_{wk-1}^b > K_{wk-1}$; $\min\{\Omega_{wk}^a, \Omega_{wk}^b\} = K_{wk}$; $\max\{\Omega_{wk}^a, \Omega_{wk}^b\} = \Omega_{wk}^\gamma$; $\Omega_{wk+1}^a, \Omega_{wk+1}^b > K_{sk}$ and therefore $I_{wk-1} \cap I_{cs} = \emptyset$ and $I_{wk} = (\Omega_{wk}^\gamma, \min\{\Omega_{wk+1}^a, \Omega_{wk+1}^b\}) \cap I_{cs} \neq \emptyset$. Thus, only the interval corresponding to the state wk partially belongs to the interval I_{cs}. It follows that the range of $m_2\delta_2$ values compatible with the requirement of complete separation in the case of strong and strong-intermediate desorbent is $\Omega_{wk}^\gamma < m_2\delta_2 < K_{sk}$.

Section 3

Necessary and sufficient conditions for section 3 can be obtained following the same arguments as for section 2. The obtained results are reported in Table 2.

Manuscript received July 9, 1993, and revision received Oct. 29, 1993.